Phospholipid/Aromatic Thiol Hybrid Bilayers

By

Chao Li

A thesis submitted to the Graduate Faculty of
Auburn University
In partial fulfillment of the
requirements for Master Degree

Auburn, Alabama
December 10, 2016

Keywords: Lipid bilayers, Self-assembling, Electrochemistry, Impedance, Atomic Force
Microscopy

Approved by

Wei Zhan, Chair, Associate Professor of Chemistry and Biochemistry
Rik Blumenthal, Associate Professor of Chemistry and Biochemistry
Anne Gorden, Associate Professor of Chemistry and Biochemistry

Abstract

Gold-supported hybrid bilayers comprising phospholipids and alkanethiols have been found to be highly useful in biomembrane mimicking as well as biosensing ever since their introduction by Plant in 1993 (Plant, A. L. Langmuir 1993, 9, 2764−2767). Generalizing the mechanism (i.e., hydrophobic/hydrophobic interaction) that primarily drives bilayer formation, we report here that such a bilayer structure can also be successfully obtained when aromatic thiols are employed in place of alkanethiols. Four aromatic thiols were studied here (thiophenol, 2-naphthalene thiol, biphenyl-4-thiol, and diphenylenevinylene methanethiol), all affording reliable bilayer formation when 1-palmitoyl-2-oleoylsn-glycero-3-phosphocholine liposomes were incubated with self-assembled monolayers of these thiols. Characterization of the resultant structures, using cyclic voltammetry, impedance analysis, and atomic force microscopy, confirmed the bilayer formation. Significant differences in electrochemical blocking and mechanical characteristics of these new bilayers were identified in comparison to their alkanethiol counterparts. Taking advantage of these new features, we present a new scheme for the straightforward biorecognition of a lipolytic enzyme (phospholipase A_2) using these phospholipid/aromatic thiol bilayers.

In order to present the thesis in a clear manner, this synopsis provides a brief summary of the chapters and contents.

Chapter 1 presents a detailed literature review on the simplified lipid bilayer membrane model systems, and the meaningfulness of my work. Additionally, a brief

introduction of cyclic voltammetry, impedance spectroscopy and atomic force microscopy are given at the end of chapter 1.

Chapter 2 describes the preparation and characterization experiments of the aromatic thiol SAMs and phospholipid/thiol hybrid bilayers.

Chapter 3 illustrates the characterization results of four aromatic thiols and their corresponding hybrid bilayers, via cyclic voltammetry, impedance analysis, and atomic force microscopy. Besides, a new method for the straightforward biorecognition of a lipolytic enzyme (phospholipase A_2) was explored by using these phospholipid/aromatic thiol bilayers.

Chapter 4 provides a summary of this research work and an outline for possible future directions that would follow this work.

Acknowledgments

I would like to express my sincere appreciation to my advisor Dr. Wei Zhan for his continuous guidance and great support to my life and study in Auburn University. Without his patience and encouragement, I could not make a significant progress at the beginning of my research. I really appreciate his generous heart and continuous trust even at some moments when I lost all confidence in myself.

I would like to give lots of thanks to my committee members, Dr. Anne Gorden, Dr. Rik Blumenthal for their help and valuable suggestions in my research and finishing of the thesis. I also would like to give special thanks to Dr. Christopher Easley for his permission to use the Gamry electrochemical impedance analyzer system and great help in my study and life at Auburn. I would like to give my deep thanks to Dr. Jimmy Mills who is a very kind and knowledgeable professor, and ready to provide his help as far as he can.

I would like to give my sincere thanks to my previous and current lab mates in Dr. Wei Zhan's group. Mr. Matt Ferguson, Mr. Mingming Wang, Ms. Qi Cui, Mr. Md. Shamim Ibqal, Mr. Zening Liu. I am very glad to have so many great lab mates in my life at Auburn. I would like to give my sincere thanks to Mr. Xiangpeng Li and Mr. Subramaniam for their help and good advice on research experiments. I also would like to give my sincere thanks to the previous and current working staff in our department: Ms. Lynn Walker, Ms. Carol Nixon, Ms. La Vonne Howard, Ms. Kiley Coan, Dr. Eta Isiorho, Dr.Stephen Swann, Dr. Kyle Willian and Ms. Beth Smith.

My greatest thanks go to my parents, my wife Mrs. Li Zhang and all my other family members for their support and encouragement throughout my life.

Table of Contents

List of Tables

List of Figures

List of Abbreviations

BLM   black lipid membranes

HBM   hybrid bilayer membrane

SAM   self-assembled monolayer

MLV   multilamellar vesicles

SUV   small unilamellar vesicles

LUV   large unilamellar vesicles

GUV   giant unilamellar vesicles

POPC   1-palmitoyl-2-oleoyl-sn-glycero-3-phophocholine

C12   1-dodecanethiol

C4   1-hexanethiol

C18   1-octadecanethiol

DPV   diphenylenevinylene methyl thioacetate

HEPES   4-(2- hydroxyethyl)piperazine-1-ethanesulfonic acid

CV   cyclic voltammetry

AC   alternating current

AFM   atomic force microscopy

SPM   scanning probe microscopy

L-B   Langmuir-Blodgett

DMT   Derjaguin−Muller−Toporov

RMS   root mean square

Chapter 1

Introduction

1.1 Simplified lipid bilayer membrane model systems

The biological cells and organelles are dynamic systems with complex but highly organized structures which are the sites of material transport, energy conversion, signal transduction and biosensing, which is enclosed by membranes that are as dynamic and complex as the cells themselves.[1] The main cell membrane constituents are lipids, proteins, carbohydrates and their complexes that assemble into lipid bilayers.[2] With different components as a whole, the cell membranes carry out different functions such as material specific transport, membrane receptor specific binding, membrane surface enzymatic activity, and cell-cell interactions. Especially, signal transductions among cells also rely on the binding events at the cell membrane surface, resulting in second messengers inside the cell and further control of intracellular processes such as protein synthesis and cell replication.[3] Thus, it is meaningful and challenging to study the structure and function of the cell membranes which are responsible for those activities since, generally, these proteins, carbohydrates and their complexes must be organized in a lipid matrix to maintain their native structures and activity. Currently, it is a serious challenge to achieve high-resolution structural information about cell membranes, because isolation and purification of these components are far from routine, regardless of assembly of these constituents. Therefore, simplified models of cell membranes have been the first subjects of intensive studies.

In general, a biological cell membrane, also called bio-membrane, often consists of a phospholipid bilayer with integral and peripheral proteins embedded and used in exchange of information and materials.[4] With hydrophobic tails and hydrophilic heads, the lipids form a fluid matrix for those proteins to embed, rotate, and diffuse for physiological functioning.[5, 6] Hence, by just using lipids, people established a range of simplified model systems to mimic the fundamental architectural element of the cell membrane and investigate membrane activity. In fact, lipid bilayers and lipid vesicles are the most popular biomimetic model systems.[7]

1.1.1 Black lipid bilayers

Mueller, P. and his coworkers,[8] first introduced their research of bilayer (black) lipid membranes (BLMs) in the early 1960s. Since then, several generations of scientists have explored these BLM systems for biophysical studies and biotechnological applications.[9-11] Nowadays, they are the most widely used experimental models of biomembranes.[7]

In general, the conventional BLMs are formed by first painting a lipid solution across a small hole on a plastic plate which separates two aqueous solutions, and then spontaneously suspending and thinning, which leads to the actual BLMs. Since then, many methods have been developed to prepare BLMs over the years.[12-15]

2
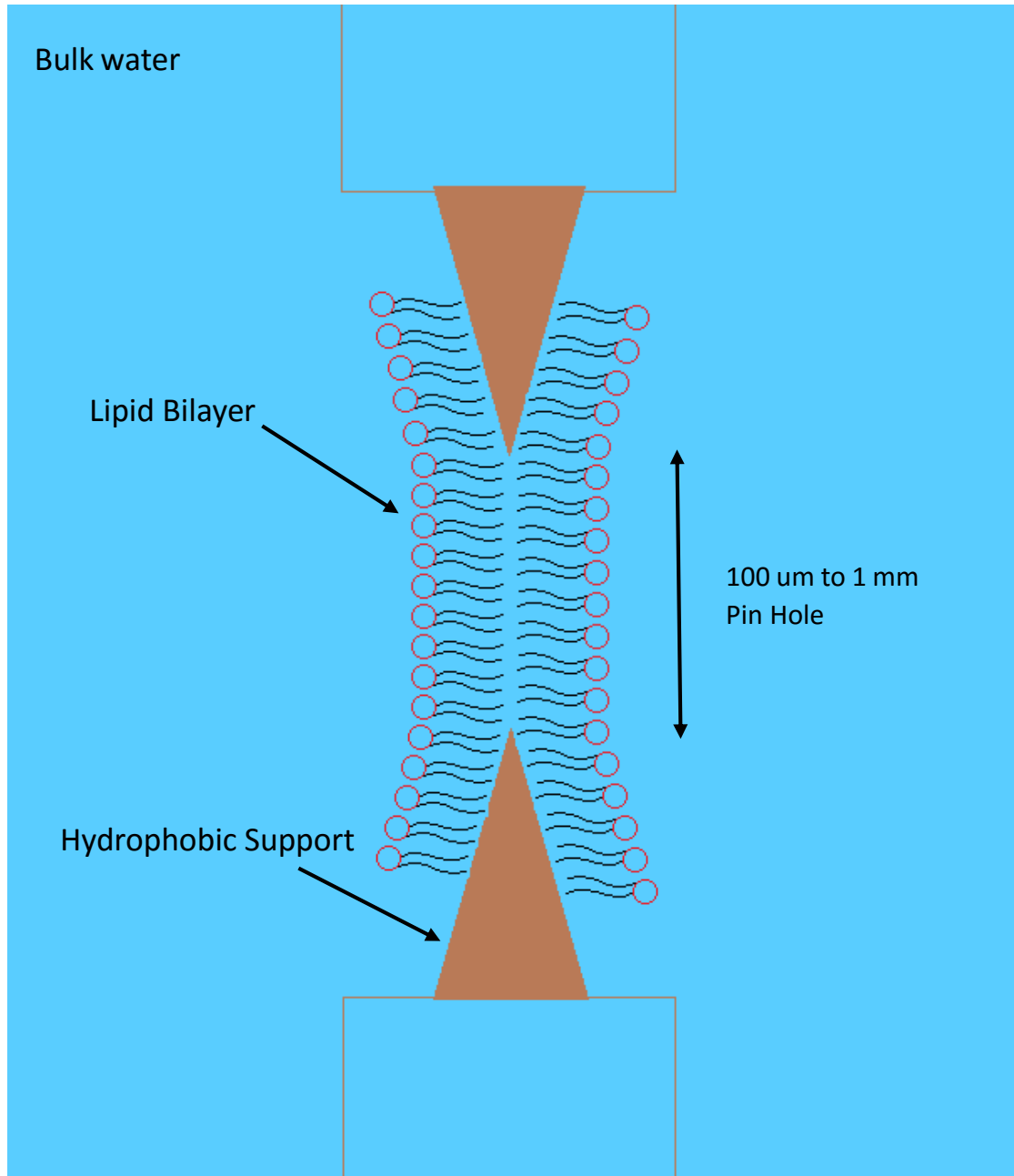
Figure 1.1 Schematic illustration of a black lipid membrane.

For example, a conventional BLM can be prepared alternatively via the Langmuir-Blodgett (L-B) technique.[2] Experimentally, a Langmuir monolayer is first formed at a surface pressure of 30−35 mN/m, which is believed to be appropriate for the lipids in bilayer membranes,[17] and then transferred from the air/water interface onto a substrate

such as a mica by slowly pulling the immersed mica sheet upward through the air/water interface. After that, the monolayer-covered mica is vertically lowered through the air/lipid monolayer/water interface and into the aqueous sub-phase to construct the lipid bilayer. Through further research, Thor D. Osborn and Paul Yager reported a formation method of planar solvent-free phospholipid bilayers via Langmuir-Blodgett transfer of monolayers to micro-machined apertures in silicon, which expands the potential value for biosensor development, receptor and drug assays, and biophysical studies of ion channels.[13]

1.1.2 Lipid vesicles

Another lipid bilayer model people often use to study bio-membrane systems is lipid vesicles (also called liposomes) which are spherical vesicles with an aqueous core surrounded by phospholipid bilayers.[18-20] According to the number of bilayers and the size variation, from very small (0.025 μm), to large (2.5 μm), to giant (10 μm), liposomes can be classified as multilamellar vesicles (MLV, with several lamellar phase lipid bilayers), small unilamellar vesicles (SUV, with one lipid bilayer), large unilamellar vesicles (LUV), and giant unilamellar vesicles (GUV), shown in figure 1.2.[21] In general, there are four steps to prepare the liposomes: first, dry lipids from organic solvents; then, disperse lipids in aqueous media to form liposomes; next, purify and collect the resultant liposomes; finally, analyze the final products.[19]

People prepare liposomes for many different applications; interestingly, the liposome application in medicine and pharmacology is one of the most widely explored

studies.[22-25] For example, liposomal drugs, which now have improved drug delivery to target particular diseased cells within the disease site and increase effectiveness of long circulation residence times, are now achieving clinical acceptance.[26-28] Moreover, studies confirmed that liposomal drugs demonstrated significantly reduced toxicities and retained enhanced efficacy on the antitumor activity compared with free drugs.[29, 30] Besides, advances in liposome design are exhibiting a particular promise as intracellular delivery systems for new biotechnology products such as antisense molecules, recombinant proteins and cloned genes.[23, 25-27, 31] Therefore, based on the pharmaceutical applications and available products, liposomes have definitely established their reputations in modern delivery systems.

Beyond their pharmaceutical aspects, another important application for liposomes, especially GUVs, is their intensive studies in different areas of biomimetic chemistry, biomembrane physics and specifically in the field of artificial cell synthesis.[21] Due to their cell-mimicking characteristics, one of the most direct applications is their use as simple comparable model systems for exploring some biological membrane physicochemical properties, for instance, mechanical properties of the vesicle membrane,[32-35] lipid "raft" or phase separation,[36-39] membrane growth,[40, 41] budding,[42-44] liposome fission[45-47] and membrane fusion.[48-51]
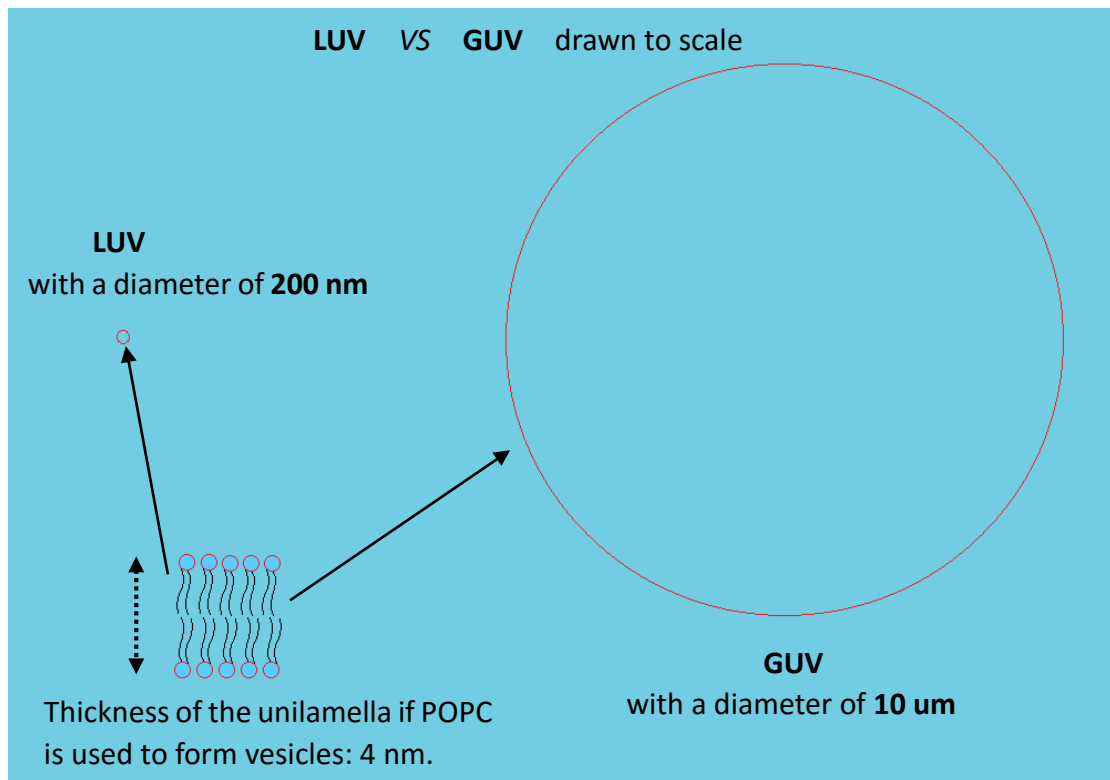
Figure 1.2 Schematic illustration of lipid vesicles.

1.1.3 Supported lipid bilayers

Furthermore, lipid bilayers formed on solid or gel substrates are called supported lipid bilayers which are a high point in lipid bilayer membrane methodologies.[2, 16, 52, 53] During the past decades, well-confined lipid bilayers have been able to be prepared on a growing number of hydrophilic substrates such as metallic wires,[54-57] microchips,[58-62] glass and oxidized silicon,[53, 63-66] with symmetrical structure and long-time stability when immersed in an aqueous medium.

6
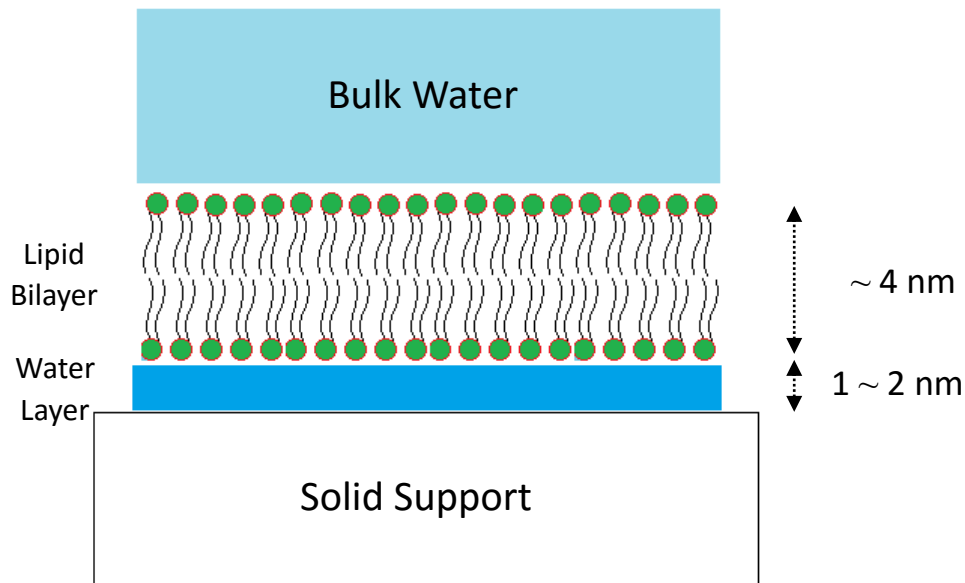
Figure 1.3 Schematic illustration of a solid supported phospholipid bilayer. The membrane is separated from the substrate by a 1~2 nm thick layer of water.

After a long development, an easier and more widely used method of supported bilayer formation is the adsorption and fusion of vesicles from an aqueous suspension to the substrate surface as Fig. 1.4 demonstrates: (1) adsorption of separate vesicles to the substrate surface; (2) fusion of vesicles on the substrate surface to form bigger vesicles; (3) rupture of the fused vesicles resulting in bilayer islands; and (4) merging of the islands to form a continuous bilayer.
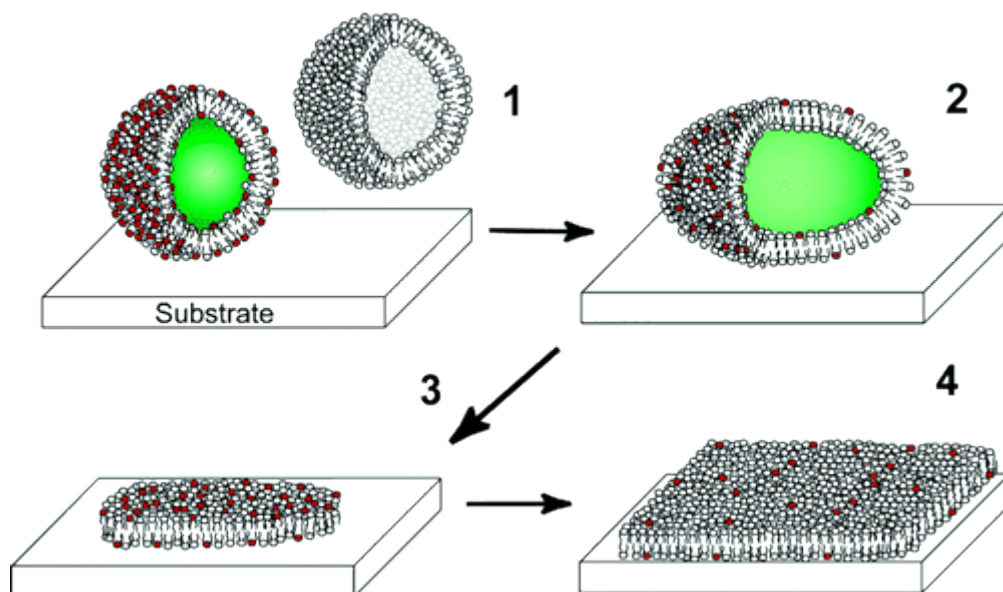
Figure 1.4 Schematic illustration of four step scenario to form supported phospholipid bilayer. Taken with permission from Ref. 63.[63]

Compared to black lipid bilayers and lipid vesicles, a big advantage of supported lipid bilayers is the significant increase in robustness and stability of the bilayer membrane. Another strength of supported lipid bilayers is that researchers could use many powerful and surface-specific analytical techniques such as atomic force microscopy,[63, 67-71] surface plasmon resonance,[72-75] quartz crystal microbalance,[76-78] vibrational sum frequency spectroscopy,[79-82] etc. to probe interactions and studies that happen at the membrane surface.

1.1.4 Hybrid lipid bilayers

After the introduction of three simple lipid bilayer membrane model systems, we can see all of them have advantages and disadvantages with respect to ease of

application and accuracy of mimicking "the real thing".[83] Phospholipid vesicles and liposomes have important uses in drug delivery and as labels in analytical applications, but few other uses for model membranes have been developed. One could imagine harnessing these insulating membranes containing receptor, enzyme, or channel proteins for applications in sensors, pharmaceutical screening, chemical synthesis, bioremediation, and separations. The technical impediments to this goal include ease of formation of the membrane, long-term integrity of the structure, and reconstitution of functional proteins in their native conformation.

In 1993, Plant A. L. first demonstrated that a monolayer of phospholipids could be reliably placed on an alkanethiol self-assembled monolayer (SAM) anchored on gold to produce a stable hybrid bilayer structure which is shown in figure 1.5.[84] While the top lipid layer reserves much utility of such structures as biomembrane mimics,[83] their direct interface with gold enables many optical, electrical, and electrochemical techniques[85-87] to be used for characterization and detection. Since then, these lipid/alkane hybrid bilayers have grown into a valuable biomembrane platform[16, 88] in fundamental as well as applied studies of lipid-based surfaces and interfaces.

Many important characteristics of phospholipid/alkane hybrid bilayers emanate from their unique formation mechanism, which is driven primarily by hydrophobic interaction between the acyl chains of lipids and the alkanethiol SAM.[83, 89] In a typical preparation of such a hybrid bilayer, a suspension of small unilamellar liposomes is incubated with a preformed SAM for a certain period of time, during which these lipid colloidal particles diffuse and adhere to the SAM, thereby rupturing and spreading to

9

eventually cover the latter as a complete monolayer. In this complex series of events, the initial energy barrier imposed by liposome rupturing is overcome by the hydrophobic interaction, and the subsequent bilayer formation is thermodynamically favored and stabilized as it not only lowers the surface energy of the aqueous-exposed hydrophobic SAM but also releases the internal mechanical stress of the curved lipid bilayer packed in the form of liposomes.[4, 90] Besides alkanethiol SAMs, the successful deposition of a monolayer of lipids on top of aqueous immersed hydrophobic surfaces has also been observed on surfaces modified with polymers,[91] silanes,[92] and ferrocene,[93] pointing to the generality of such a formation mechanism.
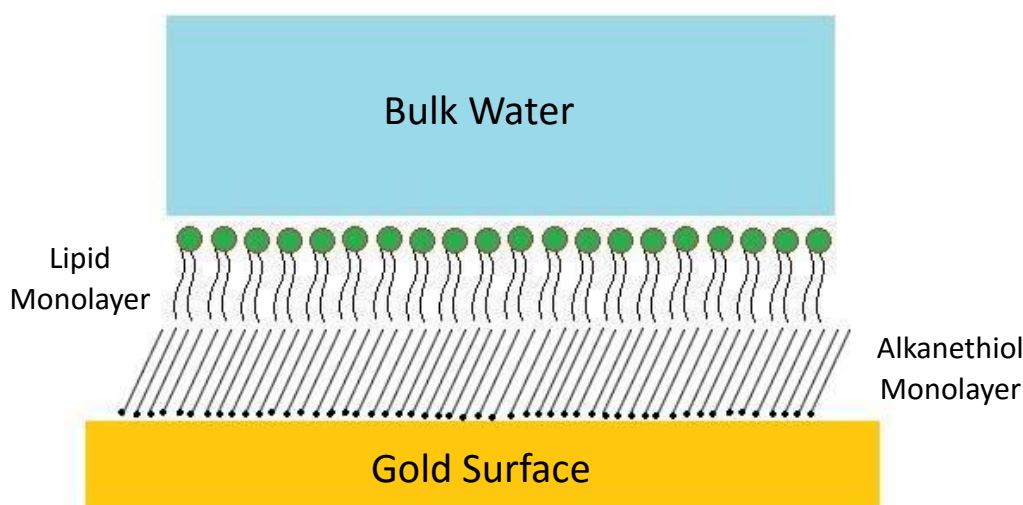
Figure 1.5 Schematic illustration of a hybrid bilayer. A single phospholipid monolayer deposits on an alkanethiol SAM.

1.2 My motivation

Generalizing the mechanism (i.e., hydrophobic/hydrophobic interaction) that primarily drives bilayer formation, my work systematically studied the deposition of phospholipids on another type of hydrophobic surface: self-assembled monolayers of aromatic thiols. Considering the differences[94-96] in size, orientation, and packing density between the SAMs formed by aromatic and alkyl thiols, we hope to identify new structural features in these aromatic/lipid based hybrid bilayers.[97] In the long term, we also envision that the prevalence of a delocalized π-electron system in aromatic thiols may potentially enhance the functionality of these hybrid lipid bilayers, e.g., on the basis of improved electrical conductivity or new electronic energy states available in such systems. Four aromatic thiols were investigated here, all of which were found to afford hybrid lipid bilayer formation.

1.3 Techniques to Characterize Hybrid Bilayer Membranes

Many techniques have been investigated to study hybrid bilayer membranes (HBMs), such as surface plasmon resonance (SPR), quartz crystal microbalance (QCM), and impedance spectroscopy.[85] Here, in this study, we mainly used cyclic voltammetry, impedance spectroscopy and and atomic force microscopy to study and characterize these hybrid bilayer membranes.

In detail, the voltammetric and impedance characteristics of these new hybrid films were compared to those of the butanethiol- and dodecanethiol-based bilayers, and atomic force microscopy (AFM) measurements of these films provide further evidence

11

of the lipid/aromatic thiol bilayer formation. A convenient voltammetric biorecognition scheme for a lipid-cleaving enzyme (phospholipase A_2) is introduced at the end, revealing important differences between aromatic- and alkane-based hybrid bilayers.

Before futher discussion of those results, it is necessary to introduce some basic backgrounds about these methods.

1.3.1 Cyclic Voltammetry

Cyclic Voltammetry (CV) is an electrochemical technique which measures the current that responds to applied electrode potential in an electrochemical cell under conditions where the potential ramps linearly versus time in cyclical phases, shown in figure 1.6. In the top panel, the potential first scans from a greater potential point a to a lower potential point d, meanwhile in the botom panel, a typical reduction signal occures during the potential scanning from a to d. Then, the reverse scan occurs from d to g, and an oxidation signal shows. Typically, CV is used to study information about electrochemical processes under various conditions, such as the presence of intermediates in oxidation-reduction reactions, the reversibility of a reaction and the reactivity of redox active species in electrolytes or bound to the electrode.[98] With the development of more sensitive detection, this method is regularly used on industrial, environmental applications and also on the pharmaceutical studies such as drug analysis in their dosage forms and especially in biological samples.[99] Specifically, in this study, it was applied to qualitatively study the insulating ability of both SAMs and HBMs on the gold electrode, which was able to indirectly confirm whether the formation of

alkanthiol SAMs or HBMs was good.

Cyclic Voltammogram Excitation Signal

Cyclic Voltammogram
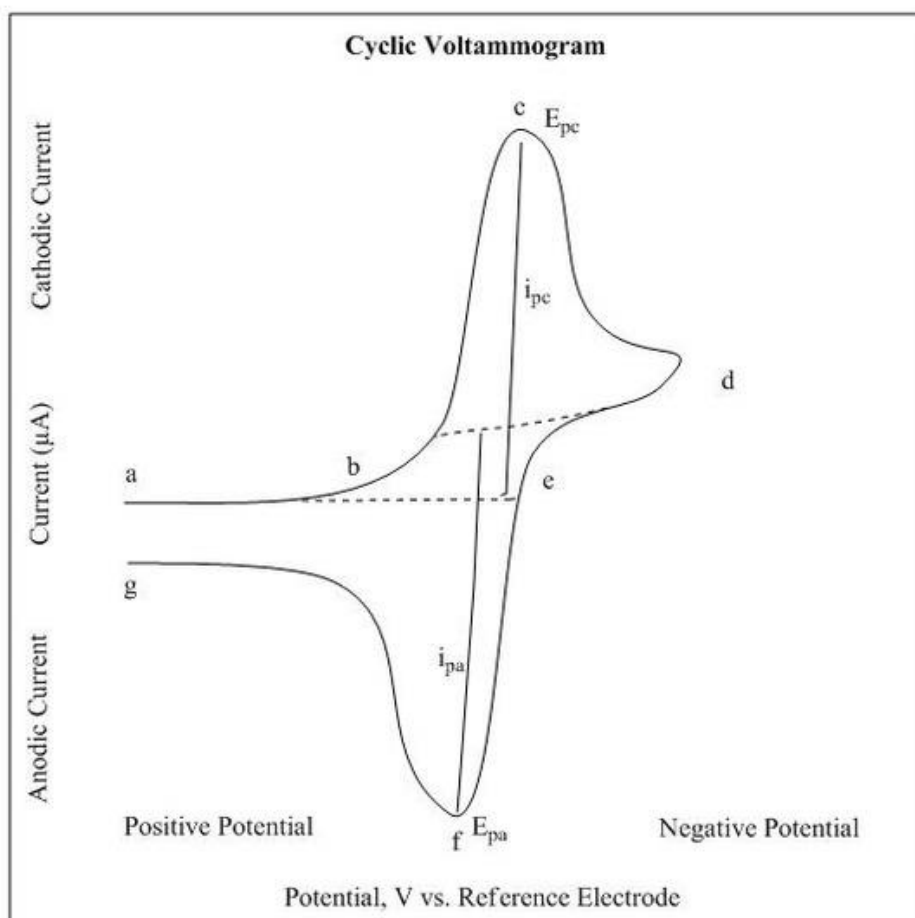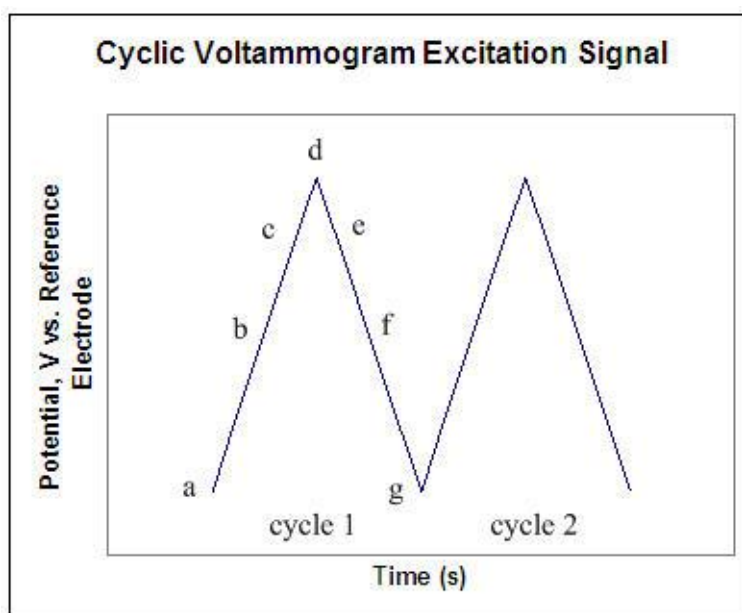
Figure 1.6 Schematic diagram of Cyclic Voltmmogram (a) applied potential scan vs. time; (b) current response vs. potential (i_{pc}, cathodic current; E_{pc}, cathodic peak potential; I_{pa}, anodic current; E_{pa}, anodic peak potential). (Ref:http://chem.libretexts.org/Core/Analytical_Chemistry/Instrumental_Analysis/Cyclic_Voltammetry)

1.3.2 Impedance Spectroscopy

Impedance is the measure of the apparent opposition presented by an alternating current (AC) circuit to the flow of alternating current when an alternating voltage is applied. In general, the impedance is consisted of two components in an AC circuit: the real part of complex impedance is formed by the normal resistance; and the imaginary part is caused by reactance. This imaginary part is composed of induction of voltages in conductors self-induced by the magnetic fields of currents (inductance), and the electrostatic storage of charge induced by voltages between conductors (capacitance). Due to the high precision, impedance techniques are widely used in lipid bilayer monitoring,[100] small molecules of biological relevance[101] and cell presence or cell concentration detection, etc.[102]

Here, in the study of HBM formation, impedance analysis is used to study hybrid lipid bilayer structure and the following changes in the surface coverage when liposomes are added to the SAM. As shown in figure 1.7, the whole system can be simplified with a solution resistance component connected in series with the membrane-associated element containing a resistance and two series capacitance

14

components configured in parallel. Without or with the top lipid monolayer, the messurement results give the capacitance values of SAMs and hybrid bilayers.
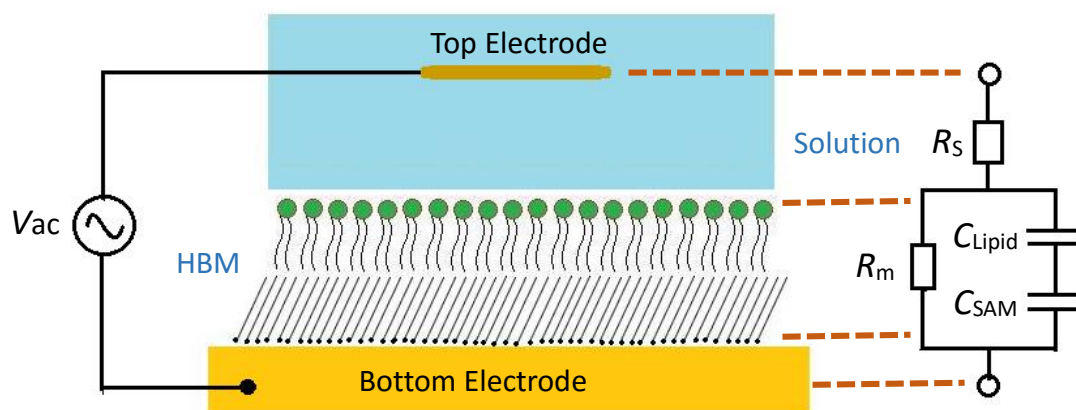
Figure 1.7 Schematic diagram and equivalent model of hybrid lipid bilayer membrane.

1.3.3 Atomic Force Microscopy

Atomic-force microscopy (AFM) is a type of scanning probe microscopy (SPM), that uses a mechanical probe to "touch" the surface extremely quickly, and is able to demonstrate a high resolution on the order of fractions of a nanometer, more than 1000 times better than the optical diffraction limit. The working principle of AFM is shown in the figure 1.8: The (x, y, z) positioning of the sample is adjusted by a piezoelectric scanner which records the position of each measurement and ensures high-precision movements; a laser beam is pointed on the top of a soft AFM cantilever and reflected to a photodiode to record tip deflection. During the moving specimen of a sample via

the scanner, the deflection signal measures the forces resulting from the interaction between the AFM tip and the sample surface with piconewton sensitivity; meanwhile, during the scanning probe on a sample, an AFM image is simulated in real time based on the height of each point of the surface.[104]

During the past 20 years, AFM has expanded exciting new opportunities for study of supported lipid bilayer membranes on the nanoscale. Particularly, AFM is well suited for the characterization of various lipid bilayer samples, because it can be conducted in liquid solution and in real time, is able to directly measure physical and mechnical properties at high resolution, and can also perturb film structure and biophysical processes in a controlled way.[105]

In this study, we used AFM to characterize the formation and structure of aromatic thiol SAMs and phospholipid/thiol hybrid bilayers and compare their mechnical properties to alkane thiol SAMs and relevant hybrid bilayers.
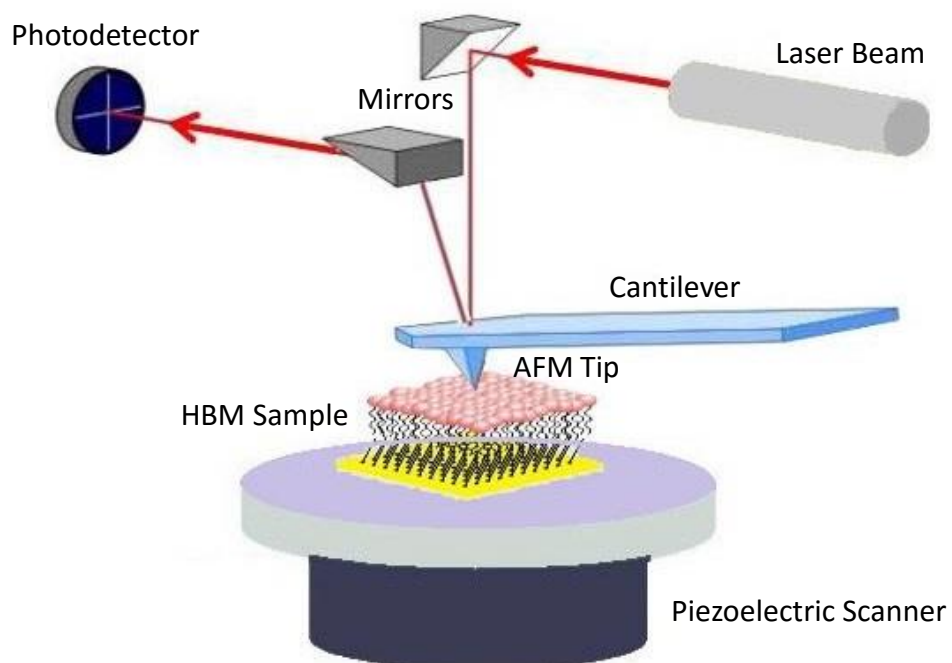
Figure 1.8 Schematic diagram of working principle of AFM.

References

1. Goni, F. M., The basic structure and dynamics of cell membranes: An update of the Singer-Nicolson model. *Biochimica Et Biophysica Acta-Biomembranes* **2014,** *1838* (6), 1467-1476.

2. Ottova, A.; Tien, H., Self-assembled bilayer lipid membranes: from mimicking biomembranes to practical applications. *Bioelectrochemistry and Bioenergetics* **1997,** *42* (2), 141-152.

3. Lautscham, L.; Lin, C.; Auernheimer, V.; Naumann, C.; Goldmann, W.; Fabry, B., Biomembrane-mimicking lipid bilayer system as a mechanically tunable cell substrate. *Biomaterials* **2014,** *35* (10), 3198-3207.

4. Schindler, T.; Kroner, D.; Steinhauser, M. O., On the dynamics of molecular self-assembly and the structural analysis of bilayer membranes using coarse-grained molecular dynamics simulations. *Biochimica Et Biophysica Acta-Biomembranes* **2016,** *1858* (9), 1955-1963.

5. Subczynski, W. K.; Wisniewska, A., Physical properties of lipid bilayer membranes: relevance to membrane biological functions. *Acta Biochimica Polonica* **2000,** *47* (3), 613-625.

6. Bagatolli, L. A.; Ipsen, J. H.; Simonsen, A. C.; Mouritsen, O. G., An outlook on organization of lipids in membranes: Searching for a realistic connection with the organization of biological membranes. *Progress in Lipid Research* **2010,** *49* (4), 378-389.

7. Eeman, M.; Deleu, M., From biological membranes to biomimetic model

membranes. *Biotechnologie Agronomie Societe Et Environnement* **2010,** *14* (4), 719-736.

8. Mueller, P.; Rudin, D. O.; Tien, H. T.; Wescott, W. C., Reconstitution of Cell Membrane Structure in vitro and Its Transformation into an excitable System. *Nature* **1962,** *194* (4832), 979.

9. Chan, Y. H. M.; Boxer, S. G., Model membrane systems and their applications. *Current Opinion in Chemical Biology* **2007,** *11* (6), 581-587.

10. Ottova, A.; Tvarozek, V.; Racek, J.; Sabo, J.; Ziegler, W.; Hianik, T.; Tien, H. T., Self-assembled BLMs: biomembrane models and biosensor applications. *Supramolecular Science* **1997,** *4* (1-2), 101-112.

11. Tien, H. T.; Ottova, A. L., From self-assembled bilayer lipid membranes (BLMs) to supported BLMs on metal and gel substrates to practical applications. *Colloids and Surfaces a-Physicochemical and Engineering Aspects* **1999,** *149* (1-3), 217-233.

12. Kalb, E.; Frey, S.; Tamm, L. K., Formation of Supported Plannar Bilayers by Fusion of Vesicles to Supported Phospholipid Monolayers. *Biochimica Et Biophysica Acta* **1992,** *1103* (2), 307-316.

13. Osborn, T. D.; Yager, P., Formation of Plannar Solvent-free Phospholipid-bilayers by Langmuir-Blodgett Transfer of Monolayers to Micromachined Apertures in Silicon. *Langmuir* **1995,** *11* (1), 8-12.

14. Bajkova, S. K.; Drychkin, A. V., Modification of Mueller's method for estimation of permeability of artificial and native bimolecular lipid membranes for steroid hormones. *Biologicheskie Membrany* **2003,** *20* (5), 419-424.

15. Heitz, B. A.; Xu, J. H.; Jones, I. W.; Keogh, J. P.; Comi, T. J.; Hall, H. K.; Aspinwall, C. A.; Saavedra, S. S., Polymerized Planar Suspended Lipid Bilayers for Single Ion Channel Recordings: Comparison of Several Dienoyl Lipids. *Langmuir* **2011,** *27* (5), 1882-1890.

16. Castellana, E. T.; Cremer, P. S., Solid supported lipid bilayers: From biophysical studies to sensor design. *Surface Science Reports* **2006,** *61* (10), 429-444.

17. Marsh, D., Lateral pressure in membranes. *Biochimica Et Biophysica Acta-Reviews on Biomembranes* **1996,** *1286* (3), 183-223.

18. Patil, Y. P.; Jadhav, S., Novel methods for liposome preparation. *Chemistry and Physics of Lipids* **2014,** *177*, 8-18.

19. Akbarzadeh, A.; Rezaei-Sadabady, R.; Davaran, S.; Joo, S. W.; Zarghami, N.; Hanifehpour, Y.; Samiei, M.; Kouhi, M.; Nejati-Koshki, K., Liposome: classification, preparation, and applications. *Nanoscale Research Letters* **2013,** *8*, 9.

20. Jesorka, A.; Orwar, O., Liposomes: Technologies and Analytical Applications. *Annual Review of Analytical Chemistry* **2008,** *1*, 801-832.

21. Walde, P.; Cosentino, K.; Engel, H.; Stano, P., Giant Vesicles: Preparations and Applications. *Chembiochem* **2010,** *11* (7), 848-865.

22. Lian, T.; Ho, R. J. Y., Trends and developments in liposome drug delivery systems. *Journal of Pharmaceutical Sciences* **2001,** *90* (6), 667-680.

23. Uchida, T.; Taneichi, M., Clinical application of surface-linked liposomal antigens. *Mini-Reviews in Medicinal Chemistry* **2008,** *8* (2), 184-192.

24. Ulrich, A. S., Biophysical aspects of using liposomes as delivery vehicles.

Bioscience Reports **2002,** *22* (2), 129-150.

25. Duzgunes, N.; Simoes, S.; Slepushkin, V.; Pretzer, E.; Flasher, D.; Salem, II; Steffan, G.; Konopka, K.; De Lima, M. C. P., Delivery of antiviral agents in liposomes. *Liposomes, Pt E* **2005,** *391*, 351-373.

26. Babai, I.; Samira, S.; Barenholz, Y.; Zakay-Rones, Z.; Kedar, E., A novel influenza subunit vaccine composed of liposome-encapsulated haemagglutinin/neuraminidase and IL-2 or GM-CSF. I. Vaccine characterization and efficacy studies in mice. *Vaccine* **1999,** *17* (9-10), 1223-1238.

27. Babai, I.; Samira, S.; Barenholz, Y.; Zakay-Rones, Z.; Kedar, E., A novel influenza subunit vaccine composed of liposome-encapsulated haemagglutinin/neuraminidase and IL-2 or GM-CSF. II. Induction of TH1 and TH2 responses in mice. *Vaccine* **1999,** *17* (9-10), 1239-1250.

28. Banerjee, R.; Tyagi, P.; Li, S.; Huang, L., Anisamide-targeted stealth liposomes: A potent carrier for targeting doxorubicin to human prostate cancer cells. *International Journal of Cancer* **2004,** *112* (4), 693-700.

29. Storm, G.; Roerdink, F. H.; Steerenberg, P. A.; Dejong, W. H.; Crommelin, D. J. A., Influence of Lipid-Composition on the Antitumor-Activity Exerted by Doxorubicin-Containing Liposomes in a Rat Solid Tumor-Model. *Cancer Research* **1987,** *47* (13), 3366-3372.

30. Mayer, L. D.; Nayar, R.; Thies, R. L.; Boman, N. L.; Cullis, P. R.; Bally, M. B., Ientification of Vesicle Propertites That Enhance the Antitumor-Activity of Liposomal Vincristine againsst Murine L1210 Leukemia. *Cancer Chemotherapy and*

Pharmacology **1993,** *33* (1), 17-24.

31. Oku, N.; Yamazaki, Y.; Matsuura, M.; Sugiyama, M.; Hasegawa, M.; Nango, M., A novel non-viral gene transfer system, polycation liposomes. *Advanced Drug Delivery Reviews* **2001,** *52* (3), 209-218.

32. Lira, R. B.; Dimova, R.; Riske, K. A., Giant Unilamellar Vesicles Formed by Hybrid Films of Agarose and Lipids Display Altered Mechanical Properties. *Biophysical Journal* **2014,** *107* (7), 1609-1619.

33. Elani, Y.; Purushothaman, S.; Booth, P. J.; Seddon, J. M.; Brooks, N. J.; Law, R. V.; Ces, O., Measurements of the effect of membrane asymmetry on the mechanical properties of lipid bilayers. *Chemical Communications* **2015,** *51* (32), 6976-6979.

34. Kato, N.; Ishijima, A.; Inaba, T.; Nomura, F.; Takeda, S.; Takiguchi, K., Effects of Lipid Composition and Solution Conditions on the Mechanical Properties of Membrane Vesicles. *Membranes* **2015,** *5* (1), 22-47.

35. Meleard, P.; Gerbeaud, C.; Bardusco, P.; Jeandaine, N.; Mitov, M. D.; Fernandez-Puente, L., Mechanical properties of model membranes studied from shape transformations of giant vesicles. *Biochimie* **1998,** *80* (5-6), 401-413.

36. Goh, S. L.; Amazon, J. J.; Feigenson, G. W., Toward a Better Raft Model: Modulated Phases in the Four-Component Bilayer, DSPC/DOPC/POPC/CHOL. *Biophysical Journal* **2013,** *104* (4), 853-862.

37. Wesolowska, O.; Michalak, K.; Maniewska, J.; Hendrich, A. B., Giant unilamellar vesicles - a perfect tool to visualize phase separation and lipid rafts in model systems. *Acta Biochimica Polonica* **2009,** *56* (1), 33-39.

38. Ostroumova, O. S.; Chulkov, E. G.; Stepanenko, O. V.; Schagina, L. V., Effect of flavonoids on the phase separation in giant unilamellar vesicles formed from binary lipid mixtures. *Chemistry and Physics of Lipids* **2014,** *178*, 77-83.

39. Haluska, C. K.; Baptista, M. S.; Fernandes, A. U.; Schroder, A. P.; Marques, C. M.; Itri, R., Photo-activated phase separation in giant vesicles made from different lipid mixtures. *Biochimica Et Biophysica Acta-Biomembranes* **2012,** *1818* (3), 666-672.

40. Takakura, K.; Toyota, T.; Sugawara, T., A novel system of self-reproducing giant vesicles. *Journal of the American Chemical Society* **2003,** *125* (27), 8134-8140.

41. Hardy, M. D.; Yang, J.; Selimkhanov, J.; Cole, C. M.; Tsimring, L. S.; Devaraj, N. K., Self-reproducing catalyst drives repeated phospholipid synthesis and membrane growth. *Proceedings of the National Academy of Sciences of the United States of America* **2015,** *112* (27), 8187-8192.

42. Li, L.; Liang, X. Y.; Lin, M. Y.; Qiu, F.; Yang, Y. L., Budding dynamics of multicomponent tubular vesicles. *Journal of the American Chemical Society* **2005,** *127* (51), 17996-17997.

43. Yu, Y.; Vroman, J. A.; Bae, S. C.; Granick, S., Vesicle Budding Induced by a Pore-Forming Peptide. *Journal of the American Chemical Society* **2010,** *132* (1), 195-201.

44. Li, J. F.; Zhang, H. D.; Qiu, F., Budding Behavior of Multi-Component Vesicles. *Journal of Physical Chemistry B* **2013,** *117* (3), 843-849.

45. Staneva, G.; Angelova, M. I.; Koumanov, K., Phospholipase A(2) promotes raft budding and fission from giant liposomes. *Chemistry and Physics of Lipids* **2004,** *129* (1), 53-62.

46. Zhou, Y. F.; Yan, D. Y., Real-time membrane fission of giant polymer vesicles. *Angewandte Chemie-International Edition* **2005,** *44* (21), 3223-3226.

47. Inaoka, Y.; Yamazaki, M., Vesicle fission of giant unilamellar vesicles of liquid-ordered-phase membranes induced by amphiphiles with a single long hydrocarbon chain. *Langmuir* **2007,** *23* (2), 720-728.

48. Zhou, Y. F.; Yan, D. Y., Real-time membrane fusion of giant polymer vesicles. *Journal of the American Chemical Society* **2005,** *127* (30), 10468-10469.

49. Sunami, T.; Caschera, F.; Morita, Y.; Toyota, T.; Nishimura, K.; Matsuura, T.; Suzuki, H.; Hanczyc, M. M.; Yomo, T., Detection of Association and Fusion of Giant Vesicles Using a Fluorescence-Activated Cell Sorter. *Langmuir* **2010,** *26* (19), 15098-15103.

50. Paleos, C. M.; Tsiourvas, D.; Sideratou, Z., Interaction of Vesicles: Adhesion, Fusion and Multicompartment Systems Formation. *Chembiochem* **2011,** *12* (4), 510-521.

51. Terasawa, H.; Nishimura, K.; Suzuki, H.; Matsuura, T.; Yomo, T., Coupling of the fusion and budding of giant phospholipid vesicles containing macromolecules. *Proceedings of the National Academy of Sciences of the United States of America* **2012,** *109* (16), 5942-5947.

52. Richter, R. P.; Berat, R.; Brisson, A. R., Formation of solid-supported lipid bilayers: An integrated view. *Langmuir* **2006,** *22* (8), 3497-3505.

53. Tamm, L. K.; McConnell, H. M., Supported Phospholipid-Bilayers. *Biophysical Journal* **1985,** *47* (1), 105-113.

54. Chiang, K. L.; Krull, U. J.; Nikolelis, D. P., Ellipsometric determination of the structure of surface-stabilized bilayer lipid membranes on silver metal. *Analytica Chimica Acta* **1997,** *357* (1-2), 73-77.

55. Snejdarkova, M.; Rehak, M.; Otto, M., Stability of bilayer lipid membranes on different metallic supports. *Biosensors & Bioelectronics* **1997,** *12* (2), 145-153.

56. Rehak, M.; Snejdarkova, M.; Otto, M., Self-assembled Lipid Bilayers as a Potassium Sensor. *Electroanalysis* **1993,** *5* (8), 691-694.

57. Tien, H. T., Self-assembled Lipid Bilayers for Biosensors and Molecular Electronic Devices. *Advanced Materials* **1990,** *2* (6-7), 316-318.

58. Teng, W.; Ban, C.; Hahn, J. H., Formation of lipid bilayer membrane in a poly(dimethylsiloxane) microchip integrated with a stacked polycarbonate membrane support and an on-site nanoinjector. *Biomicrofluidics* **2015,** *9* (2).

59. Phillips, K. S.; Kottegoda, S.; Kang, K. M.; Sims, C. E.; Allbritton, N. L., Separations in Poly(dimethylsiloxane) Microchips Coated with Supported Bilayer Membranes. *Analytical Chemistry* **2008,** *80* (24), 9756-9762.

60. Klemic, K. G.; Buck, E.; Klemic, J. F.; Reed, M. A.; Sigworth, F. J., Quartz "microchip" partitions for improved planar lipid bilayer recording of single channel currents. *Biophysical Journal* **2000,** *78* (1), 266A-266A.

61. Pantoja, R.; Sigg, D.; Blunck, R.; Bezanilla, F.; Heath, J. R., Bilayer reconstitution of voltage-dependent ion channels using a microfabricated silicon chip. *Biophysical Journal* **2001,** *81* (4), 2389-2394.

62. Tvarozek, V.; Tien, H. T.; Novotny, I.; Hianik, T.; Dlugopolsky, J.; Ziegler, W.;

Leitmannovaottova, A.; Jakabovic, J.; Rehacek, V.; Uhlar, M., Thin-film Microsystem Applcicatble in (Bio)chemical Sensors. *Sensors and Actuators B-Chemical* **1994,** *19* (1-3), 597-602.

63. Schonherr, H.; Johnson, J. M.; Lenz, P.; Frank, C. W.; Boxer, S. G., Vesicle adsorption and lipid bilayer formation on glass studied by atomic force microscopy. *Langmuir* **2004,** *20* (26), 11600-11606.

64. Kendall, E. L.; Ngassam, V. N.; Gilmore, S. F.; Brinker, C. J.; Parikh, A. N., Lithographically Defined Macroscale Modulation of Lateral Fluidity and Phase Separation Realized via Patterned Nanoporous Silica-Supported Phospholipid Bilayers. *Journal of the American Chemical Society* **2013,** *135* (42), 15718-15721.

65. Kataoka-Hamai, C.; Yamazaki, T., Induced Rupture of Vesicles Adsorbed on Glass by Pore Formation at the Surface Bilayer Interface. *Langmuir* **2015,** *31* (4), 1312-1319.

66. Kovrigina, E. A.; Kovrigin, E. L., Fluorescence of Supported Phospholipid Bilayers Recorded in a Conventional Horizontal-Beam Spectrofluorometer. *Journal of Fluorescence* **2016,** *26* (2), 379-383.

67. Benz, M.; Gutsmann, T.; Chen, N. H.; Tadmor, R.; Israelachvili, J., Correlation of AFM and SFA measurements concerning the stability of supported lipid bilayers. *Biophysical Journal* **2004,** *86* (2), 870-879.

68. Alessandrini, A.; Viero, G.; Dalla Serra, M.; Prevost, G.; Facci, P., gamma-Hemolysin oligomeric structure and effect of its formation on supported lipid bilayers: An AFM Investigation. *Biochimica Et Biophysica Acta-Biomembranes* **2013,** *1828* (2), 405-411.

69. Alessandrini, A.; Facci, P., Phase transitions in supported lipid bilayers studied by AFM. *Soft Matter* **2014,** *10* (37), 7145-7164.

70. Garcia-Arribas, A. B.; Busto, J. V.; Alonso, A.; Goni, F. M., Atomic Force Microscopy Characterization of Palmitoylceramide and Cholesterol Effects on Phospholipid Bilayers: A Topographic and Nanomechanical Study. *Langmuir* **2015,** *31* (10), 3135-3145.

71. Jurak, M.; Chibowski, E., Characteristics of a phospholipid DOPC/cholesterol bilayer based on surface free energy and its components. *Rsc Advances* **2015,** *5* (82), 66628-66635.

72. Salamon, Z.; Macleod, H. A.; Tollin, G., Surface plasmon resonance spectroscopy as a tool for investigating the biochemical and biophysical properties of membrane protein systems .2. Applications to biological systems. *Biochimica Et Biophysica Acta-Reviews on Biomembranes* **1997,** *1331* (2), 131-152.

73. Date, T.; Matsuoka, Y.; Sakamoto, N.; Serizawa, T., Unique Adsorption Behavior of Antimicrobial Poly(hexamethylenebiguanide hydrochloride) onto Solid-supported Lipid Films. *Chemistry Letters* **2012,** *41* (12), 1571-1573.

74. Melzak, K. A.; Melzak, S. A.; Gizeli, E.; Toca-Herrera, J. L., Cholesterol Organization in Phosphatidylcholine Liposomes: A Surface Plasmon Resonance Study. *Materials* **2012,** *5* (11), 2306-2325.

75. Wang, L.; Roth, J. S.; Han, X. J.; Evans, S. D., Photosynthetic Proteins in Supported Lipid Bilayers: Towards a Biokleptic Approach for Energy Capture. *Small* **2015,** *11* (27), 3306-3318.

76. Zhao, Z. L.; Ji, X. L.; Dimova, R.; Lipowsky, R.; Liu, Y. G., Viscoelasticity of Poly(ethylene glycol) Solutions on Supported Lipid Bilayers via Quartz Crystal Microbalance with Dissipation. *Macromolecules* **2015,** *48* (6), 1824-1831.

77. Montis, C.; Gerelli, Y.; Fragneto, G.; Nylander, T.; Baglioni, P.; Berti, D., Nucleolipid bilayers: A quartz crystal microbalance and neutron reflectometry study. *Colloids and Surfaces B-Biointerfaces* **2016,** *137*, 203-213.

78. Juhaniewicz, J.; Szyk-Warszynska, L.; Warszynski, P.; Sek, S., Interaction of Cecropin B with Zwitterionic and Negatively Charged Lipid Bilayers Immobilized at Gold Electrode Surface. *Electrochimica Acta* **2016,** *204*, 206-217.

79. Casford, M. T. L.; Ge, A.; Kett, P. J. N.; Ye, S.; Davies, P. B., The Structure of Lipid Bilayers Adsorbed on Activated Carboxy-Terminated Monolayers Investigated by Sum Frequency Generation Spectroscopy. *Journal of Physical Chemistry B* **2014,** *118* (12), 3335-3345.

80. Wu, H. L.; Tong, Y. J.; Peng, Q. L.; Li, N.; Ye, S., Phase transition behaviors of the supported DPPC bilayer investigated by sum frequency generation (SFG) vibrational spectroscopy and atomic force microscopy (AFM). *Physical Chemistry Chemical Physics* **2016,** *18* (3), 1411-1421.

81. Tong, Y. J.; Li, N.; Liu, H. J.; Ge, A. L.; Osawa, M.; Ye, S., Mechanistic Studies by Sum-Frequency Generation Spectroscopy: Hydrolysis of a Supported Phospholipid Bilayer by Phospholipase A(2). *Angewandte Chemie-International Edition* **2010,** *49* (13), 2319-2323.

82. Keszthelyi, T.; Hollo, G.; Nyitrai, G.; Kardos, J.; Heja, L., Bilayer Charge Reversal

and Modification of Lipid Organization by Dendrimers as Observed by Sum-Frequency Vibrational Spectroscopy. *Langmuir* **2015,** *31* (28), 7815-7825.

83. Plant, A. L., Supported hybrid bilayer membranes as rugged cell membrane mimics. *Langmuir* **1999,** *15* (15), 5128-5135.

84. Plant, A. L., Self-assembled Phospholipid Alkanethiol Biomimetic Bilayers on Gold. *Langmuir* **1993,** *9* (11), 2764-2767.

85. Silin, V. I.; Wieder, H.; Woodward, J. T.; Valincius, G.; Offenhausser, A.; Plant, A. L., The role of surface free energy on the formation of hybrid bilayer membranes. *Journal of the American Chemical Society* **2002,** *124* (49), 14676-14683.

86. Steinem, C.; Janshoff, A.; Ulrich, W. P.; Sieber, M.; Galla, H. J., Impedance analysis of supported lipid bilayer membranes: A scrutiny of different preparation techniques. *Biochimica Et Biophysica Acta-Biomembranes* **1996,** *1279* (2), 169-180.

87. Twardowski, M.; Nuzzo, R. G., Molecular recognition at model organic interfaces: Electrochemical discrimination using self-assembled monolayers (SAMs) modified via the fusion of phospholipid vesicles. *Langmuir* **2003,** *19* (23), 9781-9791.

88. Cooper, M. A., Advances in membrane receptor screening and analysis. *Journal of Molecular Recognition* **2004,** *17* (4), 286-315.

89. Hubbard, J. B.; Silin, V.; Plant, A. L., Self assembly driven by hydrophobic interactions at alkanethiol monolayers: mechanism of formation of hybrid bilayer membranes. *Biophysical Chemistry* **1998,** *75* (3), 163-176.

90. Seifert, U.; Lipowsky, R., Adhesion of Vesicles. *Physical Review A* **1990,** *42* (8), 4768-4771.

91. Elliott, J. T.; Burden, D. L.; Woodward, J. T.; Sehgal, A.; Douglas, J. F., Phospholipid monolayers supported on spun cast polystyrene films. *Langmuir* **2003,** *19* (6), 2275-2283.

92. Howland, M. C.; Sapuri-Butti, A. R.; Dixit, S. S.; Dattelbaum, A. M.; Shreve, A. P.; Parikh, A. N., Phospholipid morphologies on photochemically patterned silane monolayers. *Journal of the American Chemical Society* **2005,** *127* (18), 6752-6765.

93. Xie, H.; Jiang, K.; Zhan, W., A modular molecular photovoltaic system based on phospholipid/alkanethiol hybrid bilayers: photocurrent generation and modulation. *Physical Chemistry Chemical Physics* **2011,** *13* (39), 17712-17721.

94. Love, J. C.; Estroff, L. A.; Kriebel, J. K.; Nuzzo, R. G.; Whitesides, G. M., Self-assembled monolayers of thiolates on metals as a form of nanotechnology. *Chemical Reviews* **2005,** *105* (4), 1103-1169.

95. Frey, S.; Stadler, V.; Heister, K.; Eck, W.; Zharnikov, M.; Grunze, M.; Zeysing, B.; Terfort, A., Structure of thioaromatic self-assembled monolayers on gold and silver. *Langmuir* **2001,** *17* (8), 2408-2415.

96. Kafer, D.; Witte, G.; Cyganik, P.; Terfort, A.; Woll, C., A comprehensive study of self-assembled monolayers of anthracenethiol on gold: Solvent effects, structure, and stability. *Journal of the American Chemical Society* **2006,** *128* (5), 1723-1732.

97. Li, C.; Wang, M. M.; Ferguson, M.; Zhan, W., Phospholipid/Aromatic Thiol Hybrid Bilayers. *Langmuir* **2015,** *31* (18), 5228-5234.

98. Nicholson, R. S., Theory and Application of Cyclic Voltammetry for Measurement of Electrode Reaction Kinetics. *Analytical Chemistry* **1965,** *37* (11), 1351.

99. Farghaly, O. A.; Hameed, R. S. A.; Abu-Nawwas, A. A. H., Analytical Application Using Modern Electrochemical Techniques. *International Journal of Electrochemical Science* **2014,** *9* (6), 3287-3318.

100. Trojanowicz, M., Miniaturized biochemical sensing devices based on planar bilayer lipid membranes. *Fresenius Journal of Analytical Chemistry* **2001,** *371* (2), 246-260.

101. Bontidean, I.; Berggren, C.; Johansson, G.; Csoregi, E.; Mattiasson, B.; Lloyd, J. A.; Jakeman, K. J.; Brown, N. L., Detection of heavy metal ions at femtomolar levels using protein-based biosensors. *Analytical Chemistry* **1998,** *70* (19), 4162-4169.

102. Yang, L. J.; Li, Y. B.; Griffis, C. L.; Johnson, M. G., Interdigitated microelectrode (IME) impedance sensor for the detection of viable Salmonella typhimurium. *Biosensors & Bioelectronics* **2004,** *19* (10), 1139-1147.

103. Liu, X. W.; Li, L.; Mason, A. J., High-throughput impedance spectroscopy biosensor array chip. *Philosophical Transactions of the Royal Society a-Mathematical Physical and Engineering Sciences* **2014,** *372* (2012).

104. Morandat, S.; Azouzi, S.; Beauvais, E.; Mastouri, A.; El Kirat, K., Atomic force microscopy of model lipid membranes. *Analytical and Bioanalytical Chemistry* **2013,** *405* (5), 1445-1461.

105. Dufrene, Y. F.; Lee, G. U., Advances in the characterization of supported lipid films with the atomic force microscope. *Biochimica Et Biophysica Acta-Biomembranes* **2000,** *1509* (1-2), 14-41.

Chapter 2

Hybrid Bilayer Membrane: Preparation and Characterization

2.1 Chemicals and Reagents

1-Palmitoyl-2-oleoyl-sn-glycero-3-phosphocholine (POPC) was purchased from Avanti Polar Lipids (Alabaster, AL). Other chemicals, including potassium hexacyanoferrate(II) trihydrate ($K_4Fe(CN)_6 \cdot 3H_2O$), 1-butanethiol (C_4 thiol), 1-dodecanethiol (C12 thiol), thiophenol, biphenyl-4-thiol, 2-naphthalenethiol, 4-(2-hydroxyethyl)piperazine-1-ethanesulfonic acid (HEPES), trans-4-stilbenecarboxyaldehyde, triphenylphosphine, thioacetic acid, diethyl azodicarboxylate, and phospholipase A_2 (from honey bee venom Apis mellifera), were products of Sigma-Aldrich and used as received. All aqueous solutions employed in this study were prepared using 18.2 MΩ·cm deionized water (Millipore).

Diphenylenevinylene (DPV) methyl thioacetate was synthesized from stilbenecarboxyaldehyde and purified following the procedure reported by Dudek.[1] The identity and purity of the product were confirmed by 1H NMR and GC/MS (calculated, 268.0922; found, 268.1021).[2]

2.2 Assembling of Hybrid Bilayers

All monolayers and bilayers studied in this work were formed on gold substrates from two sources. For electrochemical and impedance analysis, the substrates were

fabricated in-house by sputtering gold (thickness: ~1000 nm as determined by quartz crystal microbalance) onto chromium-coated silicon wafers, and for the AFM measurements, gold-coated (thickness: 10 nm) glass substrates from Sigma-Aldrich were directly used. Right before the monolayer formation, these gold substrates were cleaned in piranha solution (3:1 v/v conc H_2SO_4/30% H_2O_2) for 3 or 15 min, with the latter time used for 1000-nm-thick gold-coated substrates. (Caution! Extreme care should be applied in handling the piranha solution because of its high reactivity toward organic materials.) These substrates were then thoroughly rinsed with DI water and dried with argon or nitrogen. Thus cleaned gold substrates were immediately immersed in ethanol solutions of aromatic thiols (1−5 mM) at room temperature for at least 15 h to afford monolayer formation. In the case of DPV SAM formation, an additional step was employed in which the acetate group of the DPV methyl thioacetate was first released via base hydrolysis by adding a small amount of concentrated NH_4OH in ethanol.[3] At the end of the incubation, the thiol-attached gold substrates were carefully rinsed with methanol and with DI water, dried in argon or nitrogen, and immediately assembled in various sample holders for electrochemical, impedance, or AFM measurements.

The deposition of lipids on self-assembled monolayers of aromatic thiols was achieved by incubating the monolayer in a POPC liposome solution. The liposomes were prepared by an extrusion-based method described previously[4] in which thoroughly dried POPC films were rehydrated in HEPES buffer and extruded through 400 and 80 nm polycarbonate membranes consecutively. To form a hybrid bilayer comprising

phospholipid and aromatic thiol, a certain volume of the liposome solution, with a typical POPC concentration of 2.5 mM, was gently added to an aromatic SAM fixed in the Teflon cell and incubated for 2 h. The unbound liposomes were then removed from the cell by thorough buffer (10 mM HEPES, 100 mM NaCl, pH 7.7) exchange.

2.3 Electrochemical Measurements

The electrochemical measurements were performed in homemade Teflon cells housing SAM covered gold substrates (with or without a deposited lipid layer) as the working electrode, a platinum wire as the counter electrode, and Ag/AgCl in saturated KCl solution as the reference electrode. Cyclic voltammetry of these films was operated by a PC-controlled potentiostat (CHI 910B, CH Instruments), and the scan rate was 100 mV/s. The probe solutions contained 1 mM potassium hexacyanoferrate(II) in 1 M KCl.

For the voltammetric detection of phospholipase A_2, solutions containing 10 µg/mL enzyme dissolved in 10 mM HEPES buffer saline (10 mM $CaCl_2$ and 100 mM NaCl, pH 7.7) were incubated with various SAM/lipid bilayers at room temperature for 30 min. After this step, the enzyme solutions were replaced by the same ferrocyanide solution as above, and voltammograms were then similarly obtained using gold covered with the enzyme-treated lipid films as the working electrode.

2.4 Impedance Analysis

Impedance spectroscopy measurements of aromatic thiol SAMs and the corresponding POPC/SAM hybrid structures were carried out on a Gamry

electrochemical impedance analyzer system (Reference 600). Similar to the cyclic voltammetry setup, the Teflon cells hold a gold working electrode covered with a SAM or a bilayer, a platinum counter electrode, and an Ag/AgCl reference electrode. The electrolyte solution contains 10 mM KCl in DI water. During the impedance measurement, a 10 mV ac bias was applied, and its frequency was modulated from 10 to 10^4 Hz. Thus acquired impedance data were fitted to a Randles circuit using the modeling package included in Gamry Echem Analyst, which features a solution resistance component connected in series with the membrane-associated element containing a resistance and a capacitance component configured in parallel. The fitting results give the capacitance values of SAMs and hybrid bilayers. The capacitance of the lipid monolayer can be calculated from $C_{lipid}^{-1} = C_{BL}^{-1} - C_{SAM}^{-1}$, in which C represents the capacitance values of different films.[5] The thickness of these films was estimated from the relationship $1/C = d/\varepsilon\varepsilon_0$, in which d is the thickness of the dielectric medium separating the two conducting plates (i.e., the gold electrode and the electrolyte solution) and ε is the dielectric constant of the separating medium, which is 2.3 for C_{12} thiol,[6] 2.53 for biphenyl-4-thiol,[7] 2.54 for 2-naphthalenethiol,[7] 4.26 for thiophenol,[7] and 2.7 for POPC,[6] respectively. ε_0 is the permittivity of free space ($\varepsilon_0 \approx 8.85410 \times 10^{-12}$ F m^{-1}). All standard deviations were reported from three samples, with each sample measured three times.

2.5 Atomic Force Microscopy (AFM)

A Bruker AFM system (MultiMode 8) was used for the morphological and

mechanical characterization of aromatic thiol SAMs and phospholipid/thiol hybrid bilayers. Air and fluid sample holders from the same company were used for SAM and bilayer samples, respectively. All measurements were performed at room temperature. The thickness contrast between the phospholipid top layer and the bilayer in the buffer solution was obtained by scanning a 4×4 μm^2 bilayer in which a 1×1 μm^2 POPC patch was first removed in the center. To do so, a silicon nitride cantilever (MPP 12120-10, Bruker) with a nominated spring constant of 5 N/m and resonance frequency of 150 kHz was employed. In the first scratching run, the cantilever was operated in contact mode, where a relatively large force was obtained by setting the contact mode deflection set point to 2.5−4.5 V and the scan rate to 2−4 Hz. In the second scan, the AFM was switched to tapping mode, in which a larger area was imaged with the same tip at a scan rate of 1.0 Hz. The mechanical characteristics of SAMs were probed by operating the microscope in the peak force quantitative nanomechanical mapping (QNM) imaging mode in air using another probe (ScanAsyst-Air, Bruker, spring constant 0.4 N/m, resonance frequency 70 kHz). At the beginning of each measurement, the tip was calibrated for its deflection sensitivity. Images were recorded only after the peak force curves became stable. The modulus E* was calculated by fitting the retract curve using the Derjaguin−Muller−Toporov (DMT) model.[8] All AFM images were replotted with Gwyddion software without any graphical modification or enhancement, whereas those flattened images were generated by Bruker NanoScope Analysis 1.5.

References

1. Dudek, S. P.; Sikes, H. D.; Chidsey, C. E. D. Synthesis of Ferrocenethiols Containing Oligo(phenylenevinylene) Bridges and Their Characterization on Gold Electrodes. *J. Am. Chem. Soc.* **2001**, *123*, 8033-8038.

2. Li, C.; Wang, M. M.; Ferguson, M.; Zhan, W., Phospholipid/Aromatic Thiol Hybrid Bilayers. *Langmuir* **2015,** *31* (18), 5228-5234.

3. Fan. F.-R. F.; Yao, Y.; Cai, L.; Cheng, L.; Tour, J. M.; Bard, A. J. Structure-Dependent Charge Transport and Storage in Self-Assembled Monolayers of Compounds of Interest in Molecular Electronics: Effects of Tip Material, Headgroup, and Surface Concentration. *J. Am. Chem. Soc.* **2004**, *126*, 4035-4042.

4. Zhan, W.; Jiang, K. A Modular Photocurrent Generation System Based on Phospholipid-Assembled Fullerenes. *Langmuir* **2008**, *24*, 13258-13261.

5. Plant, A. L., Self-assembled Phospholipid Alkanethiol Biomimetic Bilayers on Gold. *Langmuir* **1993,** *9* (11), 2764-2767.

6. Silin, V. I.; Wieder, H.; Woodward, J. T.; Valincius, G.; Offenhausser, A.; Plant, A. L., The role of surface free energy on the formation of hybrid bilayer membranes. *Journal of the American Chemical Society* **2002,** *124* (49), 14676-14683.

7. *CRC Handbook of Chemistry and Physics*, 85 ed.; D. R. Lide, ed., *Internet Version 2005*, <http://www.hbcpnetbase.com>, CRC Press, Boca Raton, FL, 2005.

8. Young, T. J.; Monclus, M. A.; Burnett, T. L.; Broughton, W. R.; Ogin, S. L.; Smith, P. A. The Use of the PeakForce Quantitative Nanomechanical Mapping AFM-Based

Method for High-Resolution Young's Modulus Measurement of Polymers. *Meas. Sci. Technol.* **2011,** 22, 125703.

Chapter 3

Results and findings

3.1 Characterization of Hybrid Bilayers

Four aromatic thiols are investigated in this study: thiophenol, 2-naphthalenethiol, biphenyl-4-thiol, and diphenylenevinylene (DPV) methanethiol, covering the smallest aromatic thiol (thiophenol) and three two-ring thiols of different structure and length (Figure 3.1). Compared to alkanethiols, SAMs formed by aromatic thiols often display less tilting on the gold surface, and their packing orientation also depends on the size and structure of thiols used.[1, 2] In terms of the hydrophobicity of the resulting films, water contact angle measurements made by Rubinstein and co-workers[3] showed that SAMs of several phenol thiols display significantly smaller angles as compared to SAMs formed by 1-octadecanethiol (C18 thiol). The lower packing density and association among aromatic thiols were further revealed by the observation that SAMs pre-formed by these aromatic thiols could be replaced by the C18 thiol. In the formation of a hybrid bilayer, these features may affect the deposition kinetics of lipids on these aromatic thiols as well as the mechanical, morphological, and electrical characteristics of the resulting structures. On the other hand, we chose zwitterionic 1-palmitoyl-2-oleoyl-sn-glycero-3-phosphocholine (POPC) as the single lipid component to avoid unnecessary complications at the beginning of this investigation. Owing to its low phase-transition temperature (-2 °C), the liposomal assemblies of POPC are expected to display a high fluidity at room temperature and hence a relatively low energy barrier

for spreading and fusion when exposed to a hydrophobic surface.
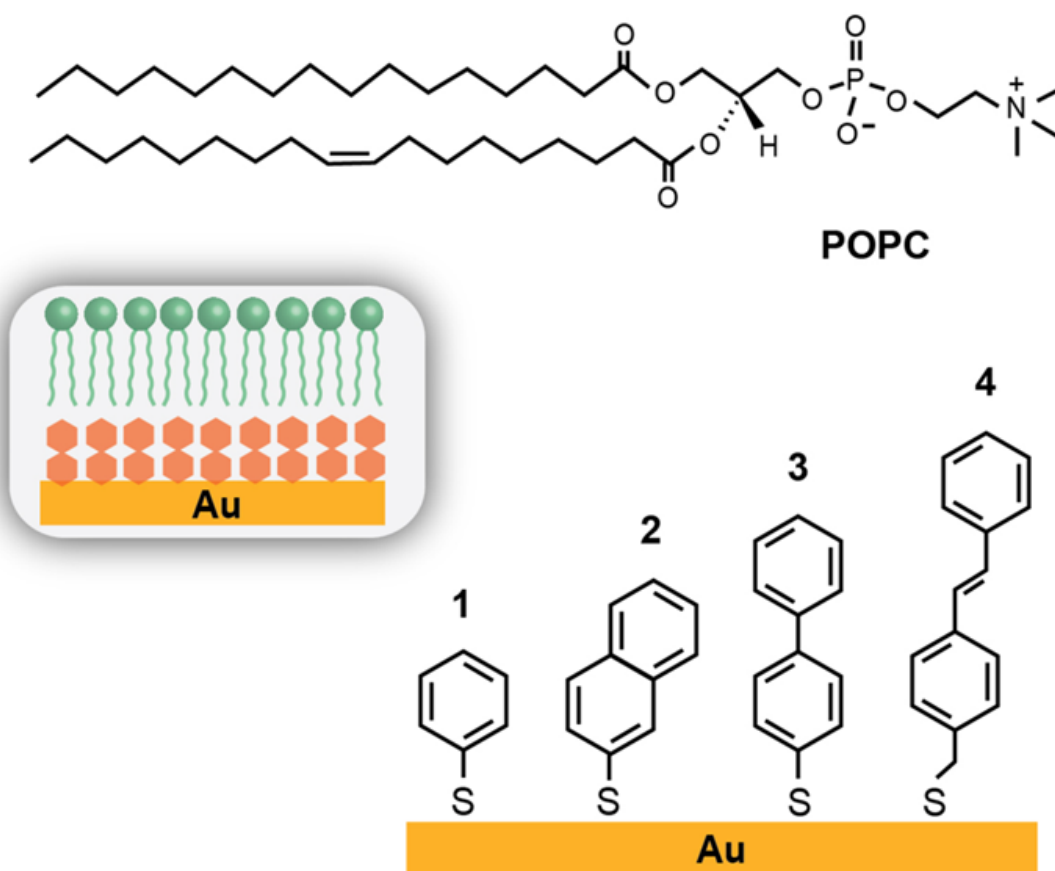

Figure 3.1 Schematic illustration of a hybrid bilayer consisting of an aromatic thiol monolayer self-assembled on a gold surface and a lipid monolayer. Aromatic thiols studied (1 to 4): thiophenol, 2-naphthalenethiol, biphenyl-4-thiol, and diphenylenevinylene methanethiol.

3.1.1 CV results

Deposition of POPC on these aromatic SAMs was achieved by the liposome fusion method similar to the preparation of lipid/alkanethiol hybrid bilayers.[5] To test the packing integrity of these aromatic SAMs as well as the corresponding lipidcontaining hybrid structures, we first examined the blocking of heterogeneous electron transfer of a small electroactive species by these films using cyclic voltammetry. As shown in Figure 3.2, because of the coverage of aromatic SAMs on the gold electrode, the oxidation of ferrocyanide in solution is significantly suppressed in all four cases. For the three shorter thiols in which the oxidation/reduction waves can still be discerned, this blocking effect is also manifested by an enlarged separation between the anodic and cathodic peaks. In comparison to results[3] on thiophenol and biphenyl-4-thiol reported by Rubinstein et al., the same SAMs presented here show a significantly stronger blocking effect, which should be due to the longer SAM formation time, i.e., overnight in our case vs 15 min to 2 h used by these authors. For SAMs alone, the degree of blocking roughly follows the size of the thiols: thiophenol < 2-naphthalenethiol < biphenyl-4-thiol < DPV.
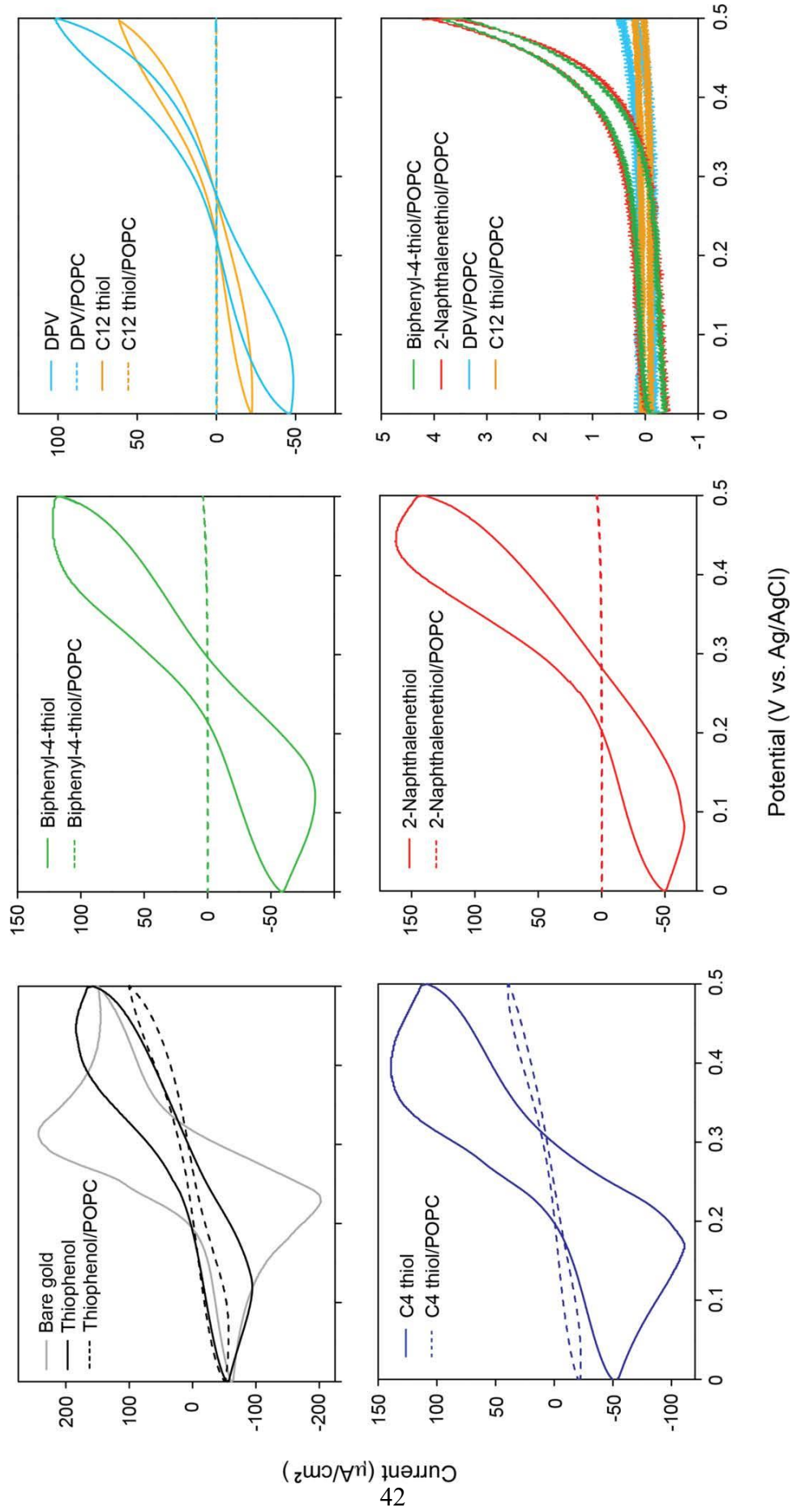
Figure 3.2 Cyclic voltammetric characterization of the formation of aromatic thiol SAMs (via the solid line) and the corresponding hybrid bilayers (via the dashed line) on gold. Voltammograms of C4- and C12-based SAMs and bilayers are also included for comparison. Also included is the CV response from the bare gold surface of the same area. All scans were conducted in 1.0 mM $Fe(CN)_6{}^{4-}$ in 1 M KCl aqueous solution, and the scan rate was 100 mV/s.

Here, even the most blocking one of this series, DPV, appears to be a less-efficient blocker than dodecanethiol (Figure 3.2, third panel), whereas the least blocking thiophenol forms still inferior barriers compared to the SAM and bilayer based on butanethiol. Interestingly, when a layer of POPC was deposited on top of these aromatic SAMs, all except the shortest thiophenol were able to block ferrocyanide oxidation nearly as well as the C12 thiol-based hybrid bilayer. These results clearly demonstrate that (1) lipids such as POPC can be equally well deposited on aromatic SAMs following the same procedure and (2) regardless of the exact structure, thus-deposited lipids form a continuous and well packed top layer that can effectively inhibit the permeation of small ions and thus move them further away from the underlying gold surface. In addition, these results reinforce previous observations[6-8] that continuous lipid layers can often form on defective, discontinuous, or curved surfaces. Underlying this high tolerance toward surface irregularities is the general and constant balance of various attractive and repulsive forces at the lipid/water interface.[9]

3.1.2 Impedance analysis results

To gain more information about the structure of the lipid layer deposited on these aromatic SAMs, we next performed electrical impedance analysis on these films. Here, the attachment of a SAM or a hybrid bilayer to the gold surface significantly modifies the capacitance at the electrode/water interface and together with the solution resistance gives rise to distinctive impedance profiles characteristic of each film. As shown in Figure 3.3, top panel, the total impedance vs ac modulation frequency profiles of the four aromatic SAMs as well as their corresponding lipid hybrid structures can all be quantitatively reproduced by the Randles circuit model. In comparison, the same data can also be reasonably well fitted with a series R (solution)−C (membrane) model, with slightly but consistently inferior goodness-of-fit values (data not shown). From the fitting, one can then obtain the capacitance values associated with these membranes (Table 3.1). Here, the capacitance of the SAM decreases as its length increases, reflecting the fact that longer thiols extend the electrolytes further away from the underlying gold surface, which is in accord with the voltammetry data. By treating these SAMs as an ideal capacitor, one can further calculate the dielectric thickness of each SAM. Moreover, as shown in Figure 3.4, by plotting the over-potential values obtained from our CV measurements versus calculated dielectric thicknesses for these three aromatic SAMs (Thiophenol, 2-Naphthalenethiol, Biphenyl-4-thiol), one can see the similar trend of the over-potential values for our aromatic SAMs follow the size of the thiols. It is consistent with the blocking effects of the aromatic SAMs for the electron transfer according to the CV results, which is that the bigger the thickness of the

aromatic SAM is, the harder to make the electron transfer. Similarly, by considering the SAM and the lipid top layer as two capacitors configured in series, one can also estimate the thickness of the POPC layer. As shown in Table 3.1, except for thiophenol, a very consistent thickness of ∼1.2 nm was obtained for the lipid top layer deposited on the SAMs of the three longer thiols, thus suggesting single lipid monolayer formation on top of these aromatic SAMs. The calculated capacitance values of the POPC layer formed on the three long aromatic SAMs, ∼1.9 $\mu F/cm^2$, are well within the range of previous reports on the same lipid, e.g., 1.76 $\mu F/cm^2$ on C18 SAM1 and 2.31 $\mu F/cm^2$ on C12 SAM.[10] The reason that such an agreement was not observed in the case of thiophenol is likely due to its small size and poor packing in the resultant SAM, which allows charge penetration and thus causes the ideal capacitor model to break down.
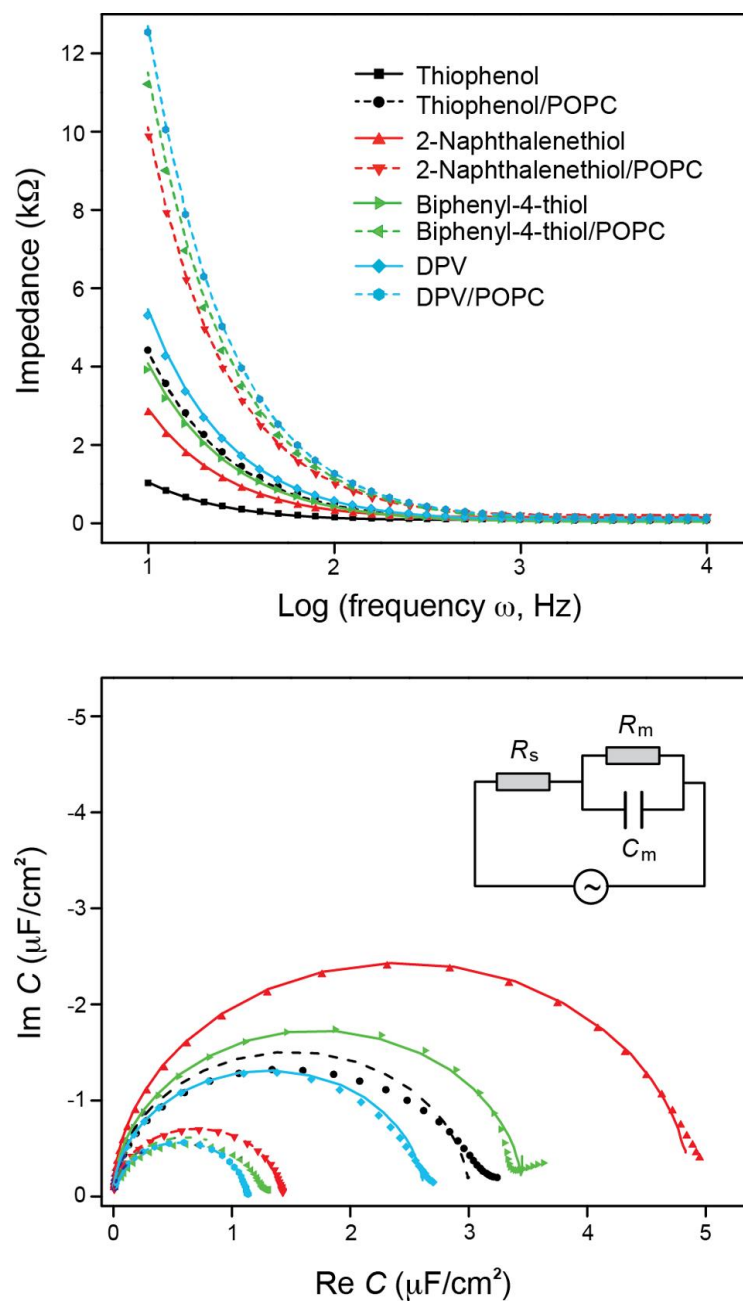
Figure 3.3 Impedance plots obtained from aromatic thiol SAMs (solid lines) and the corresponding hybrid bilayers (dashed lines) formed on gold. The supporting electrolytes contain 10 mM KCl in deionized water. The fitting results are modeled off the Randles circuit included in the figure and presented as solid/dashed lines, whereas the measured data are shown by various symbols. Not included in the bottom panel is the plot of the thiophenol SAM alone due to its significantly larger scale.

Table 3.1 Electrical capacitance values of aromatic thiol SAMs with/without POPC deposited atop.

	Capacitance and thickness of SAM (C_{SAM}, $\mu F/cm^2$ [a] and d, nm [b])	Capacitance of Bilayer (C_{BL}, $\mu F/cm^2$)[a]	Capacitance and thickness of Lipid Layer (C_{Lipid}, $\mu F/cm^2$ and d, nm) [b]
Thiophenol	13.55 ± 1.67 0.25 ± 0.01	3.12 ± 0.1	4.05 0.59
2-Naphthalenethiol	4.89 ± 0.08 0.58 ± 0.1	1.40 ± 0.04	1.96 1.22
Biphenyl-4-thiol	3.44 ± 0.09 1.16 ± 0.1	1.23 ± 0.03	1.91 1.25
DPV	2.58 ± 0.04	1.12 ± 0.04	1.96 1.22

[a]Values are obtained by fitting the impedance data with a series-RC circuit of Randle model. [b]Calculated values. See Chapter 2 for more details.
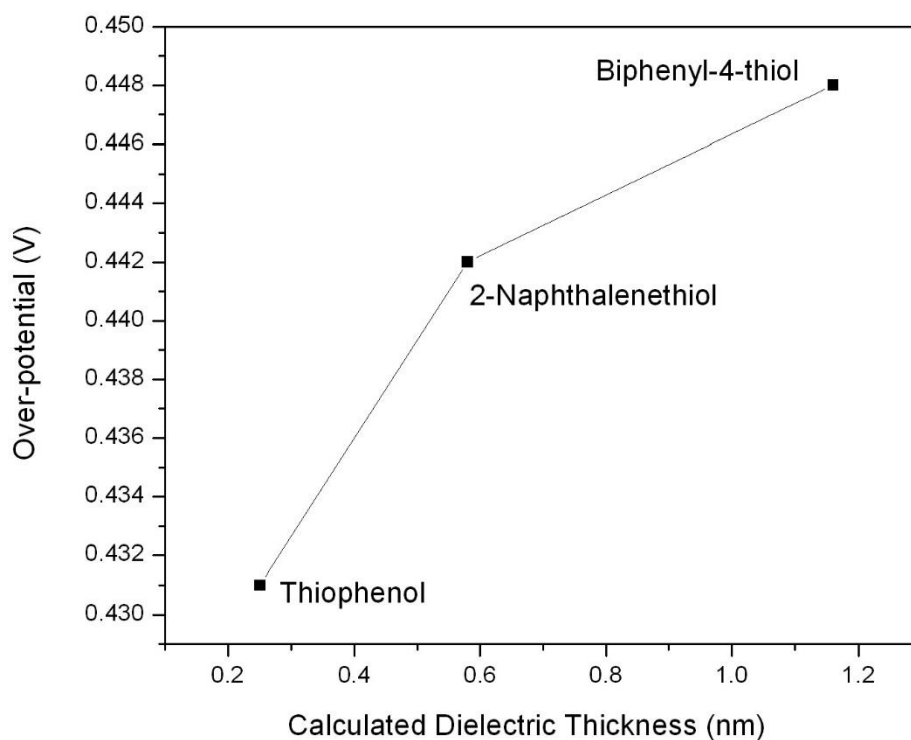
Figure 3.4 Over-potentials vs calculated dielectric thicknesses plot obtained from aromatic thiol SAMs.

In addition, plotting the real vs imaginary capacitance values associated with these films further yields the corresponding complex impedance spectra in semicircles (bottom panel, Figure 3.3). In all cases, the spectra start at the origin at high frequencies and tend to bend back and intercept the real-C axis at low frequencies, where the membrane capacitance dominates the overall impedance of the cell. The generally good agreement seen between measured and fitting data indicates that the employed circuit model adequately describes the impedance behaviors of these new hybrid bilayers, with thiophenol-based membranes again as the sole outlier.

3.1.3 AFM results

Additional evidence corroborating the above conclusion is also obtained from AFM measurement of these new hybrid structures immersed in buffer. As shown in Figure 3.5, removing the top lipid layer from the underlying 2-naphthalenethiol SAM produces a negative pattern that is approximately 1.0 nm thick (measured valley to valley from the thickness profile), which compares well with the 1.2 nm feature similarly obtained from the C12 thiol-based hybrid bilayer. The roughness of the gold substrates, which is on the order of 0.3 nm, however, prevents us from drawing more quantitative conclusions regarding their relative thickness and thus the orientation of lipids deposited on these SAMs.
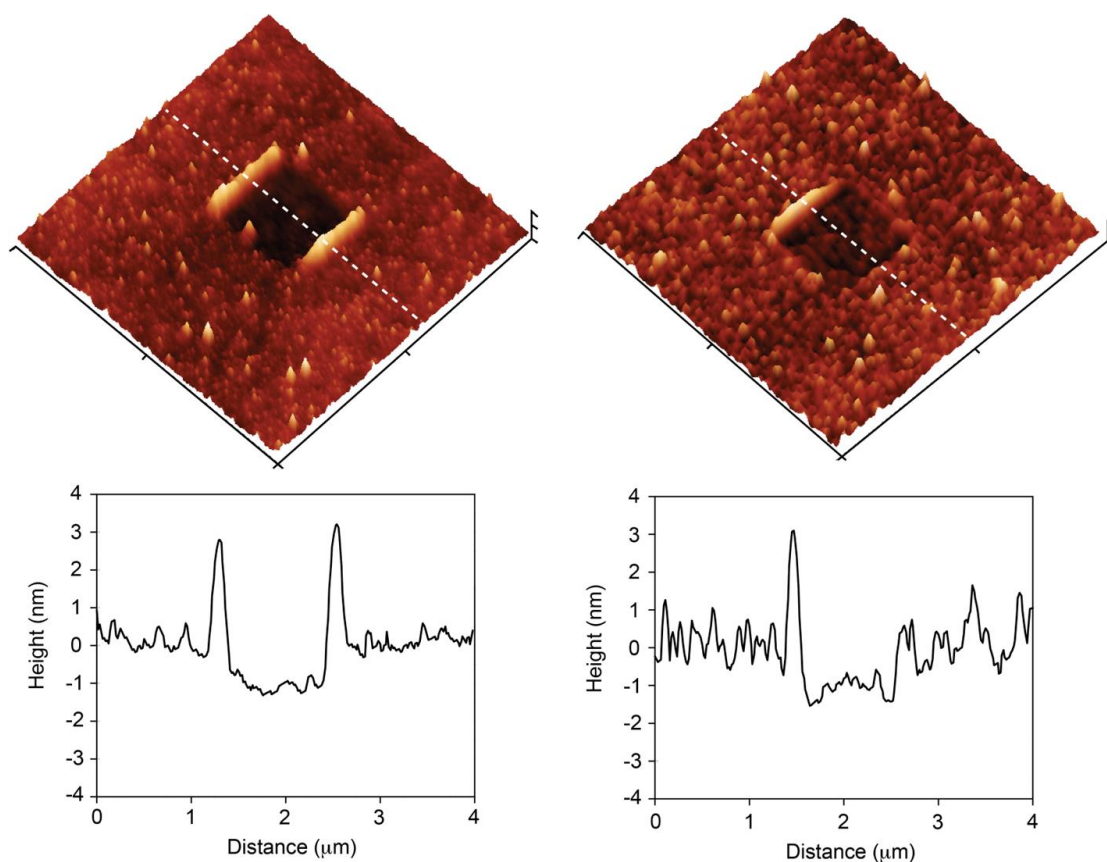
Figure 3.5 Top: AFM images of the 2-naphthalenethiol/POPC hybrid bilayer (right) as compared to that formed on the C12 SAM (left). Area scanned: 4×4 μm^2. To reveal the thickness of the top lipid layer, a 1×1 μm^2 lipid patch was first removed before imaging. See the Chapter 2 for more details. Bottom: height profiles obtained from line scans (dashed lines) across the center of the corresponding images shown at the top.

Table 3.2 Mechanical characteristics of 2-naphthalenethiol and biphenyl-4-thiol SAMs as compared to C12 SAM.

	DMT Modulus (MPa)	RMS (MPa)
2-Naphthalenethiol	374.69	23.68
Biphenyl-4-thiol	856.61	232.39
C12 thiol	1722.04	496.26

AFM nanomechanical mapping of these SAMs further revealed that a significant difference in elasticity exists among these organic thin films (Table 3.2). Of these, the C12 SAM displays the highest elastic modulus compared to the tested aromatic thiols, whereas the value associated with the biphenyl-4-thiol SAM is more than twice as high as that of 2-naphthalenethiol. These results point out the fact that the mechanical characteristics of SAMs are critically dependent on the structure, size, and packing density of the constituent thiols.

3.2 Phospholipase A₂ detection

To explore the application potential of these aromatic/lipid hybrid bilayers and particularly features that may set these new structures apart from their alkanethiol-based counterparts, we next designed and examined a biorecognition scheme in which a lipolytic enzyme, phospholipase A₂, was detected voltammetrically on these hybrid lipid bilayers.
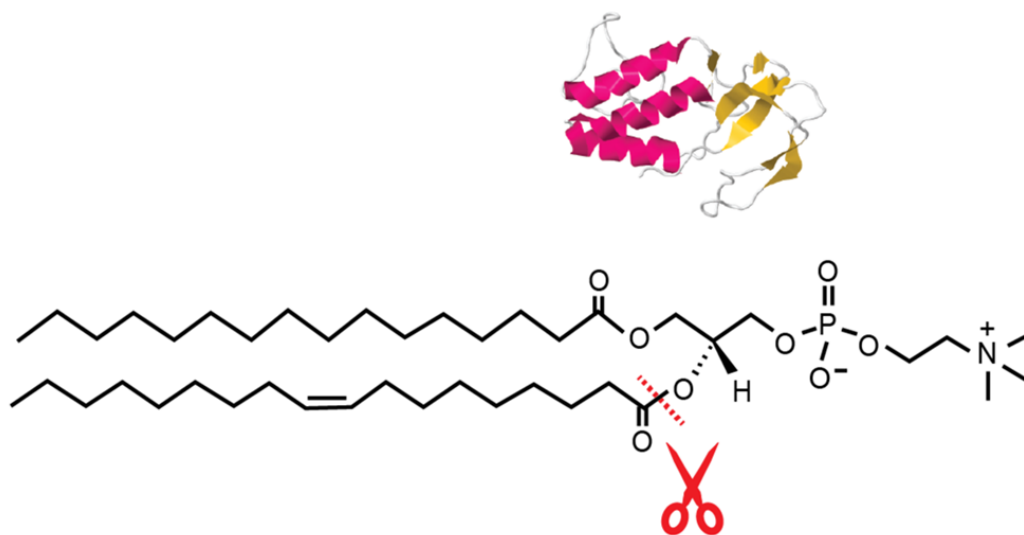
Figure 3.6 Schematic illustration of a phospholipase A₂. The structure (PDB 1POC) of this enzyme and its cleavage site on phospholipids are shown.

As shown in Figure 3.6, this enzyme specifically hydrolyzes the sn-2 acyl bond of a phospholipid, (i.e., POPC as the case here), producing its corresponding free fatty acid and lysophospholipid.[11,12] Significantly, treating the 2-naphthalenethiol/POPC bilayer with phospholipase A₂ nearly completely restores the oxidation of ferrocyanide directly obtained from the corresponding SAM alone (Figure 3.2), which demonstrates

that this enzyme can effectively hydrolyze phospholipids packed in a planar hybrid bilayer. Moreover, the accompanying cathodic wave is noticeably larger than that from the SAM alone, suggesting that the enzyme treatment produces a restructured lipid surface rather than a complete removal of the lipids from the SAM. From a biosensor's perspective, interestingly, superior sensitivity can be obtained with the aromatic/lipid bilayer as compared to its alkane/lipid counterparts. In the case of the bilayer based on butanethiol, specifically, the low sensitivity is caused by the relatively large voltammetric response from its bilayer, which translates to a large background noise. For the longer C12-based structure, on the other hand, the sensitivity is extremely poor because the film after the enzyme treatment remains almost as blocking as the starting bilayer, rendering this bilayer rather ineffective in the detection of the enzyme (Figure 3.7, voltammograms in orange). By contrast, optimal detection is achieved by the aromatic-based bilayer because as a whole this bilayer still functions as an adequate mass-transfer barrier to the redox probe in solution (i.e., low background), and more importantly, the top lipid layer contributes predominantly to the blocking of electron transfer, whose hydrolysis and restructuring thus produce a high voltammetric signal. Consequently, it is the large difference in the blocking of heterogeneous electron transfer displayed by the two types of hybrid lipid bilayers on which our biorecognition mechanism is based.
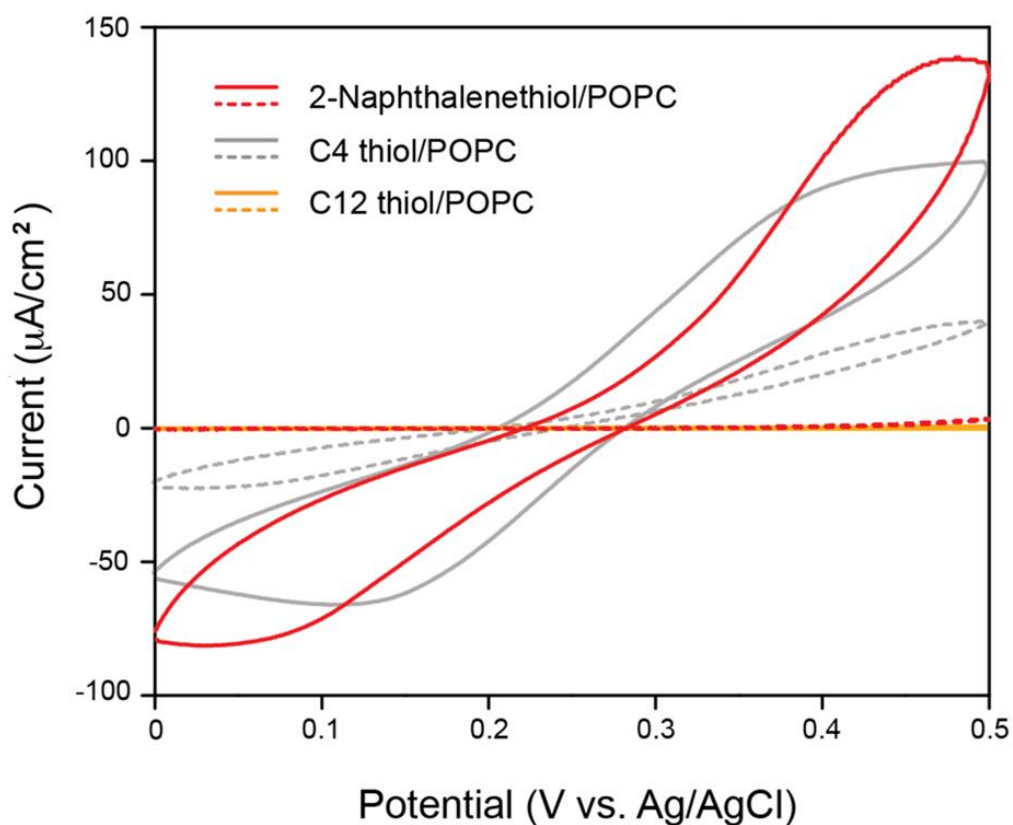
Figure 3.7 Cyclic voltammetric detection of phospholipase A$_2$ using the 2-naphthalenethiol/POPC hybrid bilayer. The CV responses were obtained from 1.0 mM Fe(CN)$_6$$^{4-}$ in 1 M KCl before (dashed line) and after (solid line) the bilayer was incubated in 10 μg/mL phospholipase A$_2$ for 30 min. The same operation was also run on the C4/POPC and C12/POPC bilayers for comparison.

The different voltammetry responses shown by the two types of hybrid bilayers are necessarily a result of some structural change in the deposited lipids caused by the enzyme treatment, which can be understood as follows. To begin with, the enzymatic hydrolysis alters the chemical and structural identities of the lipid monolayer, which break the balance of various forces at the lipid/water interface and therefore may

53

potentially trigger a morphological change and loss of material in the lipid layer. Because both reaction products are more water-soluble than the starting lipid, they display a higher tendency to leave for the aqueous phase. Considering the packing geometry, moreover, the hydrolysis converts the rod-shaped POPC for which the lamellar organization represents the most stable structure to its lysophospholipid and fatty acid, whose energetically favored assemblies are the regular and inverted micelles, respectively. Before the departure of these lipid derivatives from the lipid/water interface can occur, however, another energy price has to be paid for them to overcome the hydrophobic/hydrophobic attraction executed by the SAM underneath. Indeed, such an energy barrier can be so high for long-chained lipids that the cleaved products remain associated with the bilayer.[13] This nondeparture of lipids explains the CV of C12-based bilayers upon enzyme treatment, in which the observed oxidation current is actually less than that of its SAM alone (Figure 3.2). By contrast, the aromatic SAMs pose less hydrophobic drag toward the acyl chains of the lipids (e.g., based on contact angle measurements)[3] and hence a lower energy barrier for the lipid products to desorb from the surface. As the lipid desorption proceeds, the underlying SAM is once again directly exposed to the aqueous phase, which serves to recover the voltammetric response of the aromatic SAM itself. Our preliminary AFM imaging results shown in Figure 3.8 appear to support this analysis. While the images of POPC/ C12 SAM bilayers obtained before and after the enzyme treatment display little difference, imaging the NPT-based bilayer upon enzyme incubation consistently reveals irregular stripes that can be attributed to the partial removal of the top lipid layer. The typical height of these new

features, ~3 nm, however, is greater than the thickness of the POPC layer indicated by our lipid scratching measurements (in Figure 3.4), which could be due to either the adsorbed enzymes or the readsorption of cleaved lipids. Further examination is clearly needed in order to put our interpretation on a more robust footing.

Figure 3.8 AFM images of the POPC/C12 hybrid bilayer (top) as compared to that formed on the 2-naphthalenethiol SAM (bottom) upon incubation with 10 μg/mL phospholipase A_2 for 30 min. Area scanned: 10 x 10 μm^2. Similar to Figure 3.4, a lipid patch of 1 x 1 μm^2 was removed by the AFM tip at the center of the images as a reference point. See Chapter 2 for more details.

References

1. Love, J. C.; Estroff, L. A.; Kriebel, J. K.; Nuzzo, R. G.; Whitesides, G. M., Self-assembled monolayers of thiolates on metals as a form of nanotechnology. *Chemical Reviews* **2005,** *105* (4), 1103-1169.

2. Frey, S.; Stadler, V.; Heister, K.; Eck, W.; Zharnikov, M.; Grunze, M.; Zeysing, B.; Terfort, A., Structure of thioaromatic self-assembled monolayers on gold and silver. *Langmuir* **2001,** *17* (8), 2408-2415.

3. Sabatani, E.; Cohen-Boulakia, J.; Bruening, M.; Rubinstein, I. Thioaromatic Monolayers on Gold: A New Family of Self-Assembling Monolayers. *Langmuir* **1993**, *9*, 2974-2981.

4. Li, C.; Wang, M. M.; Ferguson, M.; Zhan, W., Phospholipid/Aromatic Thiol Hybrid Bilayers. *Langmuir* **2015,** *31* (18), 5228-5234.

5. Plant, A. L., Self-assembled Phospholipid Alkanethiol Biomimetic Bilayers on Gold. *Langmuir* **1993,** *9* (11), 2764-2767.

6. Tanaka, M.; Sackmann, E. Polymer-Supported Membranes as Models of the Cell Surface. *Nature* **2005**, *437*, 656-663.

7. White, R. J.; Ervin, E. N.; Yang, T.; Chen, X.; Daniel, S.; Cremer, P. S.; White, H. S. Single Ion-Channel Recordings Using Glass Nanopore Membranes. *J. Am. Chem. Soc.* **2007**, *129*, 11766-11775.

8. Jönsson, P.; Jonsson, M. P.; Höök, F. Sealing of Submicrometer Wells by a Shear-Driven Lipid Bilayer. *Nano Lett.* **2010**, *10*, 1900-1906.

9. Israelachvili, J. N. *Intermolecular and Surface Forces*. 3rd Ed. Elsevier Inc. Amsterdam, The Netherlands, **2011**, Chapter 20.

10. Jiang, K.; Xie, H.; Zhan, W. Photocurrent Generation from $Ru(bpy)_3^{2+}$ Immobilized on Phospholipid/Alkanethiol Hybrid Bilayers. *Langmuir* **2009,** *25*, 11129-11136.

11. Cherney, D. P.; Myers, G. A.; Horton, R. A.; Harris, J. M. Optically Trapping Confocal Raman Microscopy of Individual Lipid Vesicles: Kinetics of Phospholipase A_2-Catalyzed Hydrolysis of Phospholipids in the Membrane Bilayer. *Anal. Chem.* **2006,** 78, 6928−6935.

12. Jackman, J. A.; Cho, N.-J.; Duran, R. S.; Frank, C. W. Interfacial Binding Dynamics of Bee Venom Phospholipase A2 Investigated by Dynamic Light Scattering and Quartz Crystal Microbalance. *Langmuir* **2010,** *26*, 4103-4112.

13. Mirsky, V. M.; Mass, M.; Krause, C.; Wolfbeis, O. S. Capacitive Approach To Determine Phospholipase A_2 Activity toward Artificial and Natural Substrates. *Anal. Chem.* **1998,** 70, 3674−3678.

Chapter 4
Summary and Future Outlook

4.1 Summary

This dissertation focuses on studying the phospholipid/aromatic thiol bilayers. By replacing the alkanethiol with aromatic thiol, we have explored and established here that lipid monolayers can be reliably deposited on self-assembled aromatic thiols to give rise to a new family of hybrid bilayers.

Characterization of four aromatic thiols and their corresponding hybrid bilayers here (thiophenol, 2-naphthalene thiol, biphenyl-4-thiol, and diphenylenevinylene methanethiol), via cyclic voltammetry, impedance analysis, and atomic force microscopy, demonstrates significant differences in electrochemical properties and mechanical characteristics compared to their alkanethiol counterparts (chapter 2 and 3). However, we discovered, those aromatic thiols can still provide a hydrophobic environment for POPC liposome adsorption, rapture and formation of lipid monolayers, and regardless of the exact structure, the deposited lipids form a continuous and well packed top layer which is able to effectively block the permeation of small ions and thus move them further away from the underlying gold surface. Moreover, the impedance analysis results demonstrated that, except for thiophenol, the calculated capacitance values of the POPC layer formed on the three long aromatic SAMs, ~1.9 $\mu F/cm^2$, were well within the range of previous reports on the same lipid,[1] which indicated a fairly consistent thickness of ~1.2 nm for the single lipid monolayer

formation on top of these aromatic SAMs. In addition, direct study for the HBM structure in the aqueous buffer via AFM produced that the top lipid layer from the underlying 2-naphthalenethiol SAM was approximately 1.0 nm thick, which corresponded well to the 1.2 nm results similarly obtained from the impedance analysis.

Finally, to explore the application of these new features, we developed a new method for the straightforward biorecognition of a lipolytic enzyme (phospholipase A_2) by using these phospholipid/aromatic thiol bilayers. The experimental results have successfully demonstrated that superior sensitivity could be obtained with low background and high voltammetric signal for the aromatic/lipid bilayer, based on the biorecognition mechanism that is the large difference in the blocking of heterogeneous electron transfer displayed by the aromatic SAM alone and its hybrid lipid bilayer.

4.2 Future outlook

New biomembrane models and biorecognition strategies may be developed from these new structures by exploring the rich structural varieties and novel electronic properties of aromatic thiols. To demonstrate such possibilities, we show here that a lipolytic enzyme can be detected more sensitively using these phospholipid/aromatic thiol bilayers. However, there are still several indeterminacies and limitations. For example, the uncertainty of those new features of HBMs after phospholipase A_2 treatment (shown in Figure 3.5), which needs further examination in order to better understand and use them. Besides, there are so many lipolytic enzymes in the world. The biorecognition mechanism for these phospholipid/aromatic thiol bilayers cannot

prove the specificity for any specific enzyme, which also needs further development of our biorecognition mechanism design. For instance, we can use our phospholipid/aromatic thiol hybrid bilayers to systematically study more types of lipolytic enzymes to see if we can build a quantitative relationship between the amount of different enzymes and the change of electrochemical measurement parameters before and after enzyme treatments, such as the change of the anodic or cathodic current densities, anodic or cathodic peak potentials, over-potentials or the amount of charge transfer, etc. Similarly, we can also try to use impedance analysis method to quantitatively explore if there is a clear relationship between the amount of different enzyme additions and the change of system impedance or capacitance values before and after the enzyme treatments. Hopefully, we may construct an effective biorecognition technique for different lipolytic enzymes' detection in a quantitative way.

Moreover, in fact, HBMs are also able to play an important role to investigate electron transfer within biological membranes. For example, in 2011, our group successfully reported a photocurrent generation from the HBM based models by incorporating photo-agents either ruthenium tris(bipyridyl) complexes or monomalonic fullerenes.[2] Then, in 2012, our group reported another hybrid molecular photovoltaic system, based on fullerene C_{60} and lutein (a natural photosynthetic carotenoid pigment) which are assembled in a phospholipid/alkanethiol bilayer matrix.[3] Here, we also expect that the prevalence of a delocalized π-electron system in aromatic thiols could potentially expand the functionality of these hybrid lipid bilayers, e.g., on the basis of

61

enhanced electrical conductivity or new electronic energy states available in such systems.

Continuing along those directions, our follow-up research can be directed toward the identification of potential trends in electrochemical behaviors of bilayers based on aromatic thiols of different size and structure as well as developing these structures into new biomimicking photoconversion systems.[1-3]

References

1. Jiang, K.; Xie, H.; Zhan, W. Photocurrent Generation from Ru(bpy)$_3^{2+}$ Immobilized on Phospholipid/Alkanethiol Hybrid Bilayers. *Langmuir* **2009,** *25*, 11129-11136.

2. Xie, H.; Jiang, K.; Zhan, W., A modular molecular photovoltaic system based on phospholipid/alkanethiol hybrid bilayers: photocurrent generation and modulation. *Physical Chemistry Chemical Physics* **2011,** *13* (39), 17712-17721.

3. Liu, L.; Zhan, W., Molecular Photovoltaic System Based on Fullerenes and Carotenoids Co-assembled in Lipid/Alkanethiol Hybrid Bilayers. Langmuir 2012, 28, 4877–4882.